LOW-CYCLE FATIGUE DAMAGE IN HY-80 STEEL

by

WALTER HOLLINGSWORTH CANTRELL, LIEUTENANT, UNITED STATES NAVY

B.S., U. S. Naval Academy

(1958)

and

JACOB PETER DIDIER, Jr., LIEUTENANT, UNITED STATES NAVY

B.S., U. S. Naval Academy

(1957)

SUBMITTED IN PARTIAL FULFILLMENT OF THE REQUIREMENTS

FOR THE DEGREE OF NAVAL ENGINEER

AND THE DEGREE OF

MASTER OF SCIENCE IN NAVAL ARCHITECTURE

AND MARINE ENGINEERING

at the

MASSACHUSETTS INSTITUTE OF TECHNOLOGY

May, 1965

LOW-CYCLE FATIGUE DAMAGE IN HY-80 STEEL

by

WALTER HOLLINGSWORTH CANTRELL, LIEUTENANT, UNITED STATES NAVY

B.S., U. S. Naval Academy

(1958)

JACOB PETER DIDIER, Jr., LIEUTENANT, UNITED STATES NAVY

B.S., U. S. Naval Academy

(1957)

SUBMITTED IN PARTIAL FULFILLMENT OF THE REQUIREMENTS

FOR THE DEGREE OF NAVAL ENGINEER

AND THE DEGREE OF

MASTER OF SCIENCE IN NAVAL ARCHITECTURE

AND MARINE ENGINEERING

at the

MASSACHUSETTS INSTITUTE OF TECHNOLOGY

May, 1965

LOW-CYCLE FATIGUE DAMAGE IN HY-80 STEEL

by

Walter Hollingsworth Cantrell, Lieutenant, United States Navy

and

Jacob Peter Didier, Jr., Lieutenant, United States Navy

Submitted to the Department of Naval Architecture and Marine Engineering on 21 May 1965 in partial fulfillment of the requirements for the degree of Naval Engineer and the degree of Master of Science in Naval Architecture and Marine Engineering.

ABSTRACT

The results of a research study of methods of fatigue life prediction suitable for application to the problems encountered in HY-80 steel structures are presented. A general background to the problems of low-cycle fatigue damage analysis is given. From a study of sixteen proposed fatigue life prediction methods, six of the procedures were chosen for numerical evaluation. An experimental program generated constant axial load range data and complex load spectra data with notched specimens of material having the properties of the HY-80 steel used in naval ship construction. The experimental results were used to analyze the selected fatigue life prediction methods. Modifications were applied to the selected methods as a possible means of improving their accuracy. The method of Miner, modified to sum the cycle ratio, n_i/N_i, to 0.6, was found to provide the best overall fatigue life predictions for HY-80 steel.

Thesis Supervisor: J. Harvey Evans

Title: Professor of Naval Architecture

ACKNOWLEDGMENTS

The authors wish to express their appreciation to the staff of the Naval Alloys Division, U.S. Navy Marine Engineering Laboratory, Annapolis, Maryland, and, in particular, to Messrs. M. R. Gross and R. C. Schwab for their advice, assistance, and guidance in this endeavor, and to Mr. W. L. Williams for his encouragement.

The authors also wish to thank Professor J. Harvey Evans, Department of Naval Architecture and Marine Engineering, Massachusetts Institute of Technology, for his suggestions and continuing interest in this work.

The specimens were fabricated and the testing conducted at the U.S. Navy Marine Engineerring Laboratory, Annapolis, Maryland, under the supervision of Mr. R. C. Schwab.

The facilities of the Computation Center at the Massachusetts Institute of Technology, Cambridge, Massachusetts, were used in this study.

TABLE OF CONTENTS

LIST OF SYMBOLS

A	the value of S_i for N-1 from the straight line plot of log (S_i-S_e) versus log N
a', b', ...	constant functions of cycles to failure
a_t	material dependent exponent
B	the slope of the straight line fit of $\log(S_i-S_e)$ versus log N
b,c	stress spectrum dependent constants
C, C_s	S-N parameters
D	damage ratio
D_i	damage ratio after applying cycles at the i^{th} level
D_L	damage ratio for a unit loading spectrum
d	exponent defining the slope of the straight line fit of S-N data
E	Young's Modulus
e	exponential = 2.718282
J	total number of cycles applied at or above S_i
J_o	intercept at S_i=0 of the straight line fit to the unit loading spectrum on S_i-log J coordinates
j	slope of the straight line fit to the unit loading spectrum on S_i-log J coordinates
K,K'	loading constants
K_v	a stress concentration factor
l, l_o	crack lengths
ln	natural logarithm (base e)
log	common logarithm (base 10)

M	constant function of cycles to failure
N	cycles to failure
N_a	number of cycles to failure at S_a
N_d	number of comparison points
N_f	predicted number of cycles to fatigue failure
N_i	number of cycles to failure at the i^{th} stress level
N_{i+1}	number of cycles to failure at the (i+1) stress level
N_{LP}	number of cycles to failure, predicted
N_{LT}	number of cycles to failure, test
N_p	number of cycles to failure at the intersection of the S-log N curves
N_R	total number of cycles that may be applied at all load levels above S_e prior to failure
N_T	number of test data points
N_z	number of cycles to failure at S_z
$N_1, N_2, \ldots$	cycles to failure at levels 1,2,...
n	number of cycles applied
$n_{f,i+1}$	number of cycles of life remaining afteke failure level after i number of prestresses
n_i	number of cycles applied at the i^{th} stress level
$n_{r,i+1}$	number of cycles of life remaining after i number of prestresses
$n_1, n_2, \ldots$	number of cycles applied at levels 1,2,...
q	number of levels in a spectrum
r	linear correlation coefficient
S	stress amplitude

S_a	smallest applied stress level
S_e	endurance limit stress
S_{eo}	endurance limit stress of the virgin material
S_{fo}	ultimate tensile stress
S_i	stress amplitude at the i^{th} level in the spectrum
S_R	reduced stress of constant amplitude
S_T	total stress, residual plus external
S_z	largest stress amplitude in the loading spectrum
s,w	coefficient of a regression line
V,W	S-N parameter
x	log N
x_i	the number of load cycles applied between crack initiation and final failure
x_l	lower confidence limit for x
x_u	upper confidence limit for x
y	log S
α_i	ratio of the number of cycles applied at S_i to the total number of cycles applied in the normalized loading sequence
β	loading distribution coefficient
Γ	Gamma function
γ_i	per cent of the number of cycles to failure required to initiate cracks at the i^{th} load level
Δ	degree of conservatism
δ	invarient stress exponent
ϵ	standard error of estimate

τ	metallurgical constant
λ	ratio of S_{eo} to S_{fo}
μ_i	number of load cycles applied before crack initiation
ρ_i	probability of loading
σ_A	alternating stress
σ_F	true fracture stress
σ_G, σ_R	equivalent reversed stress
σ_M	mean stress
σ_{max}	maximum stress amplitude in a cycle
σ_{min}	minimum stress amplitude in a cycle
$\bar{\sigma}$	true stress
Σ	summation
ψ_s	modified sum of the squares
ω_i	stress interaction factor which reduces the number of cycles to failure at the i^{th} level to account for prior higher stresses
Ω	stress dependent exponent

I. INTRODUCTION

HY-80 steel was developed for use in designs requiring a high strength-to-weight ratio; however, the increase in stress levels associated with the higher strength was not accompanied by a corresponding increase in low-cycle fatigue strength. Thus, present design procedures based on yield strength as the controlling material property are being reconsidered, and the fatigue properties of the material are becoming more important in design approaches.

In the past, protection against fatigue failure was accomplished by design procedures which provided for infinite life. Such procedures, though adequate from the fatigue standpoint, are not acceptable for designs limited by weight (e.g., a submarine). The design procedures must be altered to provide for a finite fatigue life if the highest possible strength-to-weight ratio is to be obtained. Therefore, the optimum utilization of HY-80 steel requires a knowledge of the performance of the material when subjected to low-cycle fatigue damage. This knowledge can be gained from large scale-model tests [10, 32] or from an analysis of laboratory data.

It is the purpose of this paper to present the results of a study of the low-cycle fatigue behavior of HY-80 steel laboratory specimens. The study does not attempt to describe rigorously the mechanism of fatigue damage, but instead reflects an emphasis on methods of fatigue life prediction

I. INTRODUCTION

HY-80 steel was developed for use in designs requiring a high strength-to-weight ratio; however, the increase in stress levels associated with the higher strength was not accompanied by a corresponding increase in low-cycle fatigue strength. Thus, present design procedures based on yield strength as the controlling material property are being reconsidered, and the fatigue properties of the material are becoming more important in design approaches.

In the past, protection against fatigue failure was accomplished by design procedures which provided for infinite life. Such procedures, though adequate from the fatigue standpoint, are not acceptable for designs limited by weight (e.g., a submarine). The design procedures must be altered to provide for a finite fatigue life if the highest possible strength-to-weight ratio is to be obtained. Therefore, the optimum utilization of HY-80 steel requires a knowledge of the performance of the material when subjected to low-cycle fatigue damage. This knowledge can be gained from large scale-model tests [10, 12] or from an analysis of laboratory data.

It is the purpose of this paper to present the results of a study of the low-cycle fatigue behavior of HY-80 steel laboratory specimens. The study does not attempt to describe rigorously the mechanism of fatigue damage, but instead reflects an emphasis on methods of fatigue life prediction suitable for engineering application to the problems of high strength-to-weight ratio structures.

II. BACKGROUND

Accumulated fatigue damage may lead to fracture when repeated or fluctuating stresses with a maximum value less than the tensile strength of the material are applied [44]. This phenomenon can be referred to as low-cycle fatigue damage when the number of cyclic loads to failure is less than one million cycles.

The concepts and background pertinent to this study of low-cycle fatigue damage of HY-80 steel are reviewed in this section. Reviews and analyses of the complete field of low-cycle fatigue damage may be found in references [2,55,66].

An analysis of cyclic fatigue data requires a description of the stresses in the material, a definition of the stress-versus-life (S-N) curve, and a consideration of the loading variables.

The initial step in the stress analysis is the definition of the stress-strain curve. Since 1944, true stress-strain relationships have been used in fatigue testing. The shape of the true stress-strain curve changes greatly during the first few cycles and then only slightly as cyclic loading continues [18,41]. Once the stabilized cyclic state has been reached, either constant load amplitude or constant strain amplitude tests can be used for the true stress-strain relationship [4, 16,41].

Because fatigue life is strongly influenced by the value of the mean stress, several methods have been proposed that attempt to account for the effect of mean stress. These

methods include the Gerber, ellipse, Haigh-Soderberg, and modified Goodman relations. All of these methods adjust the S-N curve downward in the high-cycle region to account for the maximum possible effect of mean stress. Figure 5 of reference [29] compares the adjustment given by each of these methods. Most investigators prefer the modified Goodman relation [33, 38], while some find the method to be conservative [29]. Cina modified the Goodman diagram by using the value of the true fracture stress in lieu of the ultimate tensile strength and found very good correlation on his own and other investigators' data [4]. It has been shown that the modified Goodman relation can be used for notched specimens to give reasonably good predictions for the effect of yielding in the high stress zone at the root of a notch [22].

Many investigations indicate that fatigue behavior in the low and intermediate cyclic life range ($10\text{-}10^6$ cycles) is characterized by a straight line on log-log coordinates of stress versus life [18, 41, 66]. Using this assumption of linearity, methods have been proposed to predict the S-N curve using the results of static tension tests. One such method is based on energy considerations [12] and another is empirical [41]. Predominant among other approaches, which suggest that the best fit of fatigue data is not a straight line on a log-log plot, is the linear representation on semi-log coordinates [16, 34, 65].

In any representation of the S-N curve the portions of the curve below and above the $10\text{-}10^6$ cycles region are

difficult to define; consequently, only general descriptions of the end regions are usually given. The high-stress, low-life portion of the S-N curve is generally flat, with the flat portion of a notched specimen being shorter than that of a plain (smooth) specimen. The location of the point of inflection, i.e. the endurance limit, at the low-stress, high-life portion of the S-N curve varies with material, geometry, cyclic rate, stress spectrum shape, temperature, and prior stress history [18, 27]. If the elastic strain-versus-life curve shows a distinct curvature in the intermediate cycle range, the endurance limit can be defined with extensive high-cycle test data [41]. Quicker and less accurate approximations to the endurance limit can be made with graphical methods [65] or estimates from known data [42]. The difficulty of defining the endurance limit has led some authors to suggest that the stress associated with 10^7 cycles be arbitrarily taken as the endurance limit when making fatigue calculations.

The methods of testing must be considered when evaluating cyclic test data. If the applied stresses are within the elastic range of the material, there appears to be little or no difference between tests based on controlled strain limits and those based on controlled stress limits, if conducted in the high life range [18]. In the low life range, however, plastic strain predominates, indicating that the best results should be obtained from controlled strain limit tests [41, 18].

The order of application of stress levels, the type of stress, and the stress range are test variables which alter test results. In a given stress spectrum, the application of the higher stress levels first leads to a specimen life which differs from that obtained by applying the lower stress levels first [16, 55, 63]. Pulsating-tension stresses produce a higher fatigue limit than do alternating tension-compression stresses [4]. In axial tests and bending tests of both notched and smooth specimens, life predictions based on the axial tests are usually smaller than those based on bending test results [1,16]. The reduction of fatigue life increases with increasing maximum stress and stress range. In spectrum loading tests, stress levels below the endurance limit have been observed to shorten life [64]. For sub-endurance stresses, it is felt that there exists a stress level below which cracks and damage cease to propagate [15].

Rate of cycling must be considered as a load variable. At frequencies less than 1000 cycles per minute, the fatigue life decreases with a decrease in cyclic rate [16, 18]. For ferritic steels specifically, the smaller the number of cycles between successive rest periods, the more marked is the increase in life [7, 30]. As mean stress is increased, the shape of the load-time curve plays a stronger role [18].

Other considerations which should be included when analyzing cyclic fatigue test data are stress and strain concentrations, residual stresses, size effects, environmental

The order of application of stress levels, the type of stress, and the strain range are test variables which affect test results. In a given stress sequence, the application of the higher stress levels first leads to a fatigue life which differs from that obtained by applying the lower stress levels first [16, 55, 59]. Pulsating-tension stresses produce a higher fatigue limit than do alternating tension-compression stresses [9]. In axial tests and bending tests of both notched and smooth specimens, life predictions based on the axial tests are usually smaller than those based on bending test results [1,15]. The reduction of fatigue life increases with increasing maximum stress and stress range. In successive loading tests, stress levels below the endurance limit have been observed to shorten life [44]. For sub-endurance stresses, it is felt that there exists a stress level below which cracks and damage cease to propagate [15].

Rate of cycling must be considered as a load variable. At frequencies less than 1000 cycles per minute, the fatigue life decreases with a decrease in cyclic rate [16, 13]. For periodic rest specifically, the smaller the number of cycles between successive rest periods, the more marked is the increase in life [9, 50]. As mean stress is increased, the shape of the load-time curve plays a stronger role [15].

Other considerations which should be included when comparing cyclic fatigue test data are stress and strain concentrations, residual stresses, size effects, environmental effects, surface conditions, pre-stressing, and creep. The relative degree of influence of each of these variables on fatigue life is not fully understood at this time.

Several methods for the prediction of fatigue life have been proposed in the literature by various authors. All of these methods are fundamentally the concept of gradual accumulation of fatigue damage during the progress of loading. Each author emphasizes a particular aspect or formula for the representation of either or both the applied loading spectra or the S-N data. A brief description of each of these methods, presented alphabetically by author, is given below.

1. Corten and Dolan's Method [6]

Corten and Dolan developed a non-linear cumulative damage theory in terms of stress ratios of the various loads in the spectrum. The method is based on a concept of relating fatigue damage to the number of cracks formed as a function of the largest varying load in the sequence. The growth of such cracks is assumed to occur at all load levels of the sequence. This form indicates that stresses below the endurance limit contribute damage.

2. Freudenthal and Heller's Method [14]

Freudenthal and Heller's procedure requires the construction of a "fictitious" S-N curve by the use of a stress interaction factor. To derive the stress interaction factor, a statistical analysis is performed on a

large number of samples tested under various spectra of loading. The result is a quasi-linear rule of cumulative damage which accounts for the damaging effect of low-stress amplitudes when mixed with infrequent high-stress amplitudes. Under varying stress amplitudes, this method eliminates the effect of endurance limit as a significant design value.

3. Fuller's Method [16]

Fuller analyzed the available fatigue data from many sources to arrive at an empirical approach to the failure prediction problem. The resulting method applies to loadings which have many repetitions of blocks of stress levels and permits a limited degree of random application of loading sequence within each block. Stresses below the endurance limit are considered to contribute damage.

4. Gatts' Method [17]

Gatts describes the accumulation of fatigue damage with stress amplitude as a random time function having a specific amplitude distribution. The stress amplitude distribution may be continuous or discrete. Solutions of a differential equation relating damage accumulation to the amplitude distribution of stress are used to predict fatigue life of material subjected to random loading. Damage is assumed to accumulate when the applied stress exceeds the endurance limit.

5. Grover's Method [21]

Grover's method is essentially the same as Langer's method which is described in paragraph 7 below.

6. Henry's Method [27]

Henry developed a non-linear description of the accumulation of damage. The method requires a knowledge of the order of load application and the original S-N curve. The allowable S-N curve is reduced in a step-by-step procedure by using cycle ratio corrections to account for damage by prior loadings. The cycle ratios reflect the effects of increased local stress concentrations for loading cycles at levels above the endurance limit.

7. Langer's Method [33]

Langer's method requires experimental S-N data which separate the crack initiation stage from the crack growth stage. The two resulting S-N curves are used with a linear accumulation of cycle ratios to derive a prediction of fatigue life.

8. Levy's Method [35]

Levy's procedure uses empirical constants derived from test data as exponents for each cycle ratio of a step spectrum and as a constant loading coefficient in the life prediction equation. Thus for a loading spectrum of q steps, the solution of (q+1) simultaneous equations and as many sets of test data are required.

9. Lundberg's FFA Method [39]

Lundberg, in conjunction with a group at the Aeronautical Research Institute of Sweden (FFA), represented the applied loading spectrum and allowable S-N data as mathematical formulas. These formulas were used with the assumption of linear cumulative damage to obtain a closed form solution for the predicted fatigue life.

10. Manson's Method [42]

Manson's method is applicable to cyclic bending loadings. The method assumes that the S-log N curves of a material having varying amounts of pre-stress will intersect the S-log N curve of the original material at a common point. The value of N at the point of intersection is used as a characteristic constant in the prediction of remaining fatigue life. The procedure accounts for the order dependence of load application and for the reduction in endurance limit due to pre-stressing.

11. Marco and Starkey's Method [43]

Marco and Starkey developed a method of defining damage boundaries which had been suggested by the earlier work of Kommers [31]. Kommers analyzed two-step load tests of steel coupons and pointed out the essential non-linearity of the damage boundaries. He hypothesized that the damage boundaries were functions of both the load levels and the cycle ratios in each load level. Marco and Starkey used a power relation of the cycle ratio to define the damage boundary. By making the

exponent stress (or load) dependent, a mathematical formulation resulted which can be used in the procedure previously developed by Richart and Newmark [53].

12. Miner's Method [45]

This well-known linear cumulative damage hypothesis was originally proposed by Palmgren with no basis in theory [49]. Miner later restated the hypothesis based on the following energy assumptions: (a) the amount of internal work absorbed by the material during each load cycle is constant at a given load level, (b) the maximum amount of internal work that can be absorbed from cyclic loads before failure is always the same, and (c) the amount of internal work absorbed at each load level is linearly cumulative and independent of the sequence of loading. Failure is hypothesized when the summation of the fractions of fatigue damage expressed as cycle ratio, $(\frac{n}{N})$, is equal to unity.

13. Richart and Newmark's Method [53]

Richart and Newmark developed a formal procedure for utilizing Kommer's non-linear damage hypothesis as stated in paragraph 11 above. The resulting method describes damage boundaries which vary with both stress level and the cycle ratio.

14. Shanley's "1X" and "2X" Methods [53,59,60]

Shanley's "1X" method utilizes a mathematical formula for the S-N curve and a concept of rate of forma-

tion of slip bands to derive an equation which results in the linear cumulative damage expression of Palmgren and Miner. Shanley's "2X" method is a non-linear form of the summation of fatigue damage fractions based on essentially the same concepts as his linear "1X" method. In his "2X" method one of the coefficients in the rate equation is assumed to be stress dependent, thereby greatly increasing the rate of crack growth.

15. Smith's Residual Stress Method [61]

Smith used Miner's linear cumulative damage hypothesis and an elaborate stress analysis to include the residual stresses from plastic yielding at higher load levels with the stresses from external loads.

16. Valluri's Method [62,62]

Valluri assumes that a number of cracks are generated by cyclic stresses and that final failure is due to the growth of a "dominant crack". The dominant crack is assumed to grow intermittently through active and dormant periods. The method traces the crack from its initial size to the point at which the applied maximum stress is sufficient to propagate the crack to failure. The description of cumulative damage is accomplished by converting the damage at different stress levels to damage at a reference stress level and invoking the conditions for failure at the reference stress level. The method accounts for order of application of stress in two-step

loading, but not in random loading. Stresses below the endurance limit are not considered to contribute damage. Validity of the method is claimed for the low-cycle range only.

loading, but not in random loading. Stresses below the endurance limit are not considered to contribute damage, validity of the method is claimed for the low-cycle range only.

III. OBJECTIVES

The objectives of this research study are:

1. To develop S-N characteristics for HY-80 steel from constant load range laboratory tests.
2. To develop fatigue life data from laboratory specimens subjected to complex loading spectra representative of actual HY-80 structure loading histories.
3. To compare and select proposed methods of low-cycle fatigue life prediction suitable for engineering applications to HY-80 steel structures.
4. To evaluate the selected methods of fatigue life prediction with the experimental data.
5. To provide modifications which improve the accuracy of the fatigue life prediction methods.

IV. PROCEDURE

V-notch test specimens were manufactured from steel having the properties of the HY-80 steel used in naval ship construction. The specimens were subjected to axial push-pull loadings. Complete descriptions of the specimens, the properties of the steel, and the characteristics of the testing machine are given in Appendix A.

Loading schedules were developed from stress cycle combiuations furnished by the Bureau of Ships. Descriptions of the loading schedule and resulting stress spectra are given in Appendix B.

Constant load-range tests were performed to establish the S-N curve of the material. The behavior of the material when subjected to load spectra was established with variable load-range tests. A test was terminated if a specimen survived 100,000 cycles without failure.

Sixteen proposed methods of fatigue life prediction were selected and reviewed for applicability to this study. Appendix C contains a brief description of the procedure employed by each method.

Six of the sixteen proposed methods were chosen for evaluation with the experimental data. Lack of applicability or special data precluded the evaluation of the remaining ten methods. Variations and modifications to the evaluated methods were applied where possible. The selection, application, and modification of the life prediction methods are described

IV. PROCEDURE

Eighty test specimens were manufactured from steel having the properties of the HY-80 steel used in naval ship construction. The specimens were subjected to axial push-pull loadings. Complete descriptions of the specimens, the properties of the steel, and the characteristics of the testing machine are given in Appendix A.

Loading schedules were developed from stress cycle conditions furnished by the Bureau of Ships. Descriptions of the loading schedule and resulting stress spectra are given in Appendix B.

Constant load-range tests were performed to establish the S-N curve of the material. The behavior of the material when subjected to load spectra was established with variable load-range tests. A test was terminated if a specimen survived 100,000 cycles without failure.

Sixteen proposed methods of fatigue life prediction were selected and reviewed for applicability to this study. Appendix C contains a brief description of the procedure employed by each method.

Six of the sixteen proposed methods were chosen for evaluation with the experimental data. Lack of applicability or special data precluded the evaluation of the remaining ten methods. Variations and modifications to the evaluated methods were applied where possible. The selection, application, and modification of the life prediction methods are described in Appendix D.

Each stress condition within the test spectra was converted to an equivalent reversed stress for use in evaluating the failure prediction methods. Appendix E shows the procedure for computing the equivalent stress.

Computer programs were written for the stress conversion and for each of the six chosen methods. The programs were used to generate numerical results with which to compare the methods. Comparisons were made by determining a degree of conservatism and a standard error of estimate for each method. The mathematical methods used for comparison and analysis are explained in Appendix E.

V. RESULTS

1. S-N Curves

Ten of thirteen specimens failed in the tests designed to establish the shape of the S-N curve. A linear regression analysis of the ten data points results in a linear log S-log N curve represented by the following equation:

$$SN^{0.1250465} = 181,603 \qquad (1)$$

The linear correlation coefficient, r, of the above equation is 0.976, and the standard error of estimate of N on S is 8,729 cycles.

The curves corresponding to 95 per cent confidence limits for equation (1) are described by

$$\text{(Upper)} \quad SN^{0.1250465} = 199,565 \qquad (2)$$

$$\text{(Lower)} \quad SN^{0.1250465} = 164,977 \qquad (3)$$

The curves described by equations (1), (2), and (3) are shown in Figure I.

A linear regression analysis of the same data shows the best-fit line on S-log N coordinates to be

$$\text{Log } N = -0.00006544913\ S + 7.7945125 \qquad (4)$$

The linear correlation coefficient, r, of equation (4) is 0.985, and the standard error of estimate of N on S is 6,866 cycles.

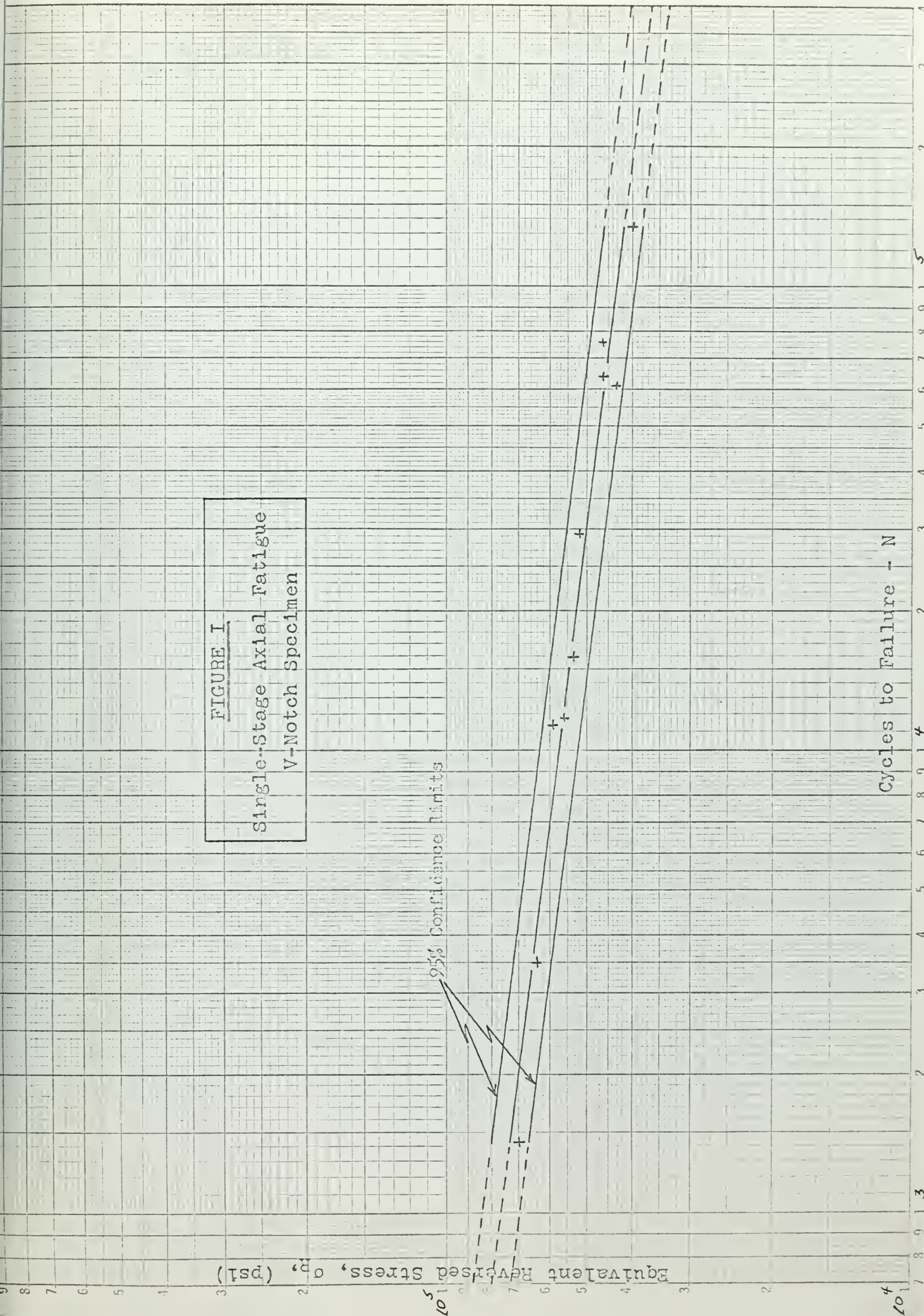
FIGURE I
Single-Stage Axial Fatigue
V-Notch Specimen
95% Confidence Limits
Cycles to Failure - N
Equivalent Reversed Stress, σ_R, (psi)
10^3
10^4
10^5

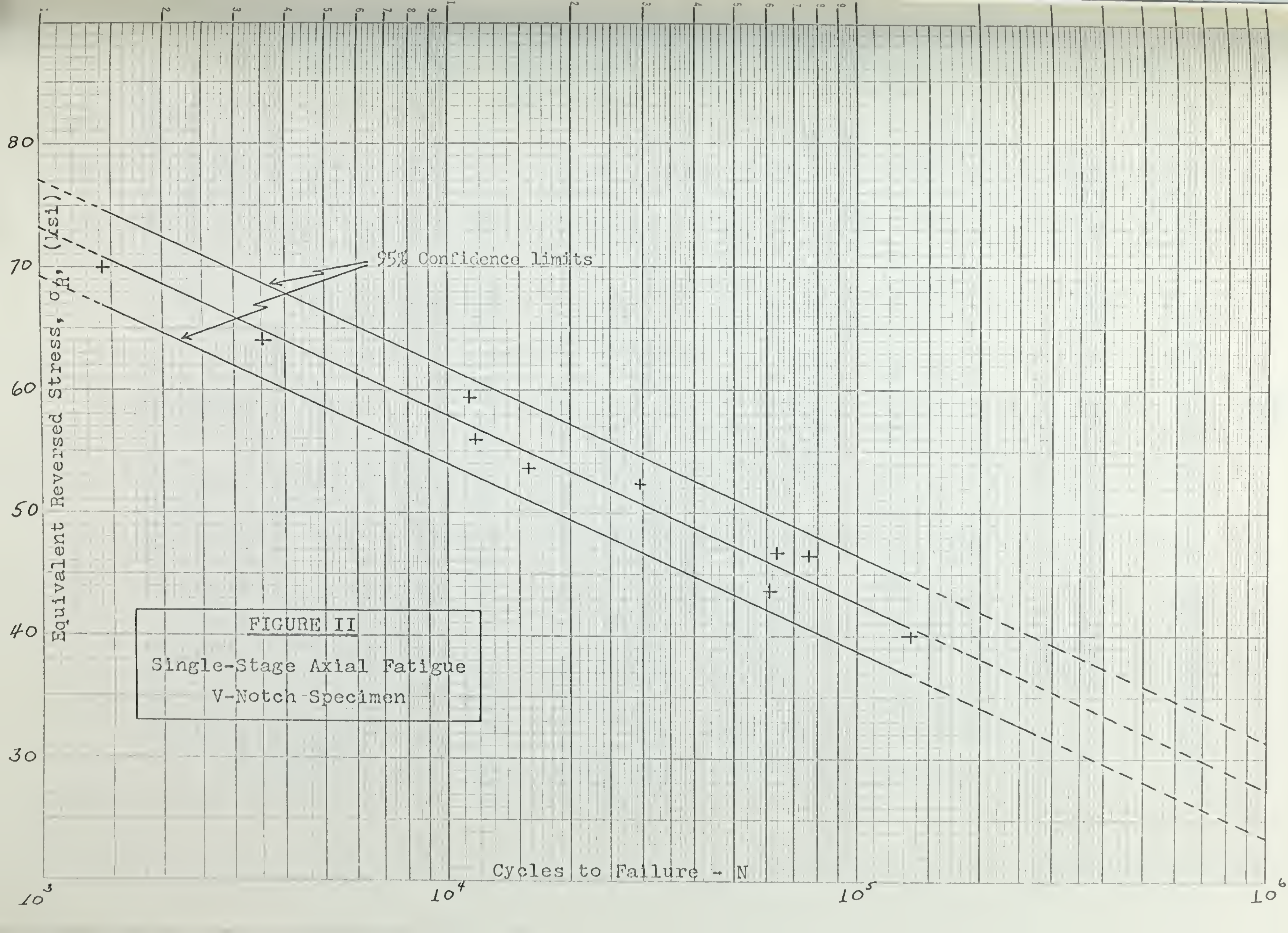

FIGURE II

Single-Stage Axial Fatigue
V-Notch Specimen

The 95 per cent confidence limit curves for equation (4) are described by

$$\text{(Upper)} \quad \text{Log } N = -0.00006544913\, S + 8.0568407 \qquad (5)$$

$$\text{(Lower)} \quad \text{Log } N = -0.00006544913\, S + 7.5321843 \qquad (6)$$

Equations (4), (5), and (6) are plotted in Figure II.

Estimation methods indicate an endurance limit stress of 52,000 psi for smooth (unnotched) HY-80 steel and 17,000 psi for notched HY-80 steel.

2. Fatigue Life Prediction Methods

Three of the 28-level spectra and six of the five-level spectra produced failures in specimens and provided a basis for comparison of the life prediction methods.

From the sixteen fatigue life prediction methods considered, the proposed methods of Miner, Fuller, Corten and Dolan, Gatts, Shanley, and Manson were selected as applicable to this study.

The standard error of estimate and degree of conservatism for each of the evaluated methods are shown in Table I and Figure III. Figure III is a graphical representation of Table I. Results obtained by evaluating a proposed method without modifications are indicated by an "A" in the identifier number column. Results not marked by an "A" correspond to evaluations performed with various modifications applied to the proposed methods. Table I shows the values of the variable parameters for which each method was evaluated.

The 95 per cent confidence limit curves for equation (4) are described by

$$\text{(Upper)} \quad \text{Log } N = -0.00004(S-40000) + 6.005517 \qquad (5)$$

$$\text{(Lower)} \quad \text{Log } N = -0.00004(S-44000) + 5.521607 \qquad (6)$$

Equations (4), (5), and (6) are plotted in Figure II.

Estimation methods indicate an endurance limit stress of 52,000 psi for smooth (unnotched) RR-50 steel and 17,000 psi for notched RR-50 steel.

2. <u>Fatigue Life Prediction Methods</u>

Three of the 24-level spectra and six of the fifty-level spectra produced failures in specimens and provided a basis for comparison of the life prediction methods.

From the sixteen fatigue life prediction methods considered, the proposed methods of Miner, Valluri, Corten and Dolan, Gatts, Shanley, and Henry were selected for evaluation in this study.

The standard error of estimate and degree of conservatism for each of the evaluated methods are shown in Table I and Figure III. Figure III is a graphical representation of Table I. Results obtained by evaluating a proposed method without modifications are indicated by an "O" in the identifier number column. Results not marked by an "O" correspond to evaluations performed with various modifications applied to the proposed methods. Table I shows the values of the variable parameters for which each method was evaluated.

Table I also lists the separate values of standard error of estimate demonstrated by eaċh method under five-level, 28-level, and all loadings.

TABLE I

STANDARD ERROR OF ESTIMATE

and

DEGREE OF CONSERVATISM

Identifier Number	Curve Form	Endurance Limit	Variable Parameters	Standard Error of Estimate (Cycles) 28 Level Spectra	5 Level Spectra	All Spectra	Degree of Conservatism All Spectra
FULLER'S METHOD							
1A	S	No		22,924	25,783	24,867	1.176
2	S	Yes		29,494	25,783	27,077	1.283
3	L	No		93,206	35,281	61,038	0.793
4	L	Yes		15,364	35,281	30,142	1.072
SHANLEY'S "2X" METHOD							
5	S	Yes		14,606	52,341	43,560	0.880
6	S	No		16,994	52,341	43,849	0.921
7A	L	Yes		16,526	57,097	47,586	0.938
8	L	No		19,860	57,097	48,009	0.982
GATTS' METHOD							
9A	S	Yes		14,751	43,520	36,540	0.967
10	L	Yes		16,614	43,636	36,897	1.043
MANSON'S METHOD							
11A	S	No	N_p=100	42,755	78,277	68,514	0.590
12	L	No	N_p=100	41,081	97,980	83,442	0.585
MINER'S METHOD							
13A	S	No	Sum=1.0	45,474	74,471	69,998	0.57
14	S	Yes	Sum=1.0	45,721	79,471	70,052	0.57
15	L	No	Sum=1.0	43,868	99,859	85,378	0.576
16	L	Yes	Sum=1.0	43,868	99,859	85,378	0.576
17	S	No	Sum=0.6	13,345	31,637	26,947	0.951
18	S	Yes	Sum=0.6	13,417	31,637	26,968	0.95

TABLE I, Continued

MINER'S METHOD, continued							
19	L	No	Sum=0.6	13,519	44,179	36,907	0.951
20	L	Yes	Sum=0.6	13,519	44,179	36,907	0.951
21	S	No	Sum=0.57	13,723	28,177	24,332	1.000
22	L	No	Sum=.576	13,894	40,920	34,360	1.000
CORTEN and DOLAN'S METHOD							
23A	S	No	δ=1.0898	34,039	21,426	26,311	1.492
24	S	Yes	δ=1.0898	32,252	21,426	25,550	1.451
25	S	Yes	δ=3.25	14,225	46,108	38,533	0.913
26	L	No	δ=7.0	35,664	89,567	75,974	0.625
27	L	Yes	δ=4.0	13,679	55,083	45,663	0.876

Notes:

1. "A" in Identifier Number column designates results of the author's unmodified method.
2. "S" in Curve Form column indicates that S-N data was on S-log N coordinates.
3. "L" in Curve Form column indicates that S-N data was on log S-log N coordinates.
4. "No" in Endurance Limit column represents S_e=0.
5. "Yes" in Endurance Limit column represents S_e= 17,000 psi.

FIGURE III

STANDARD ERROR OF ESTIMATE
and
DEGREE OF CONSERVATISM

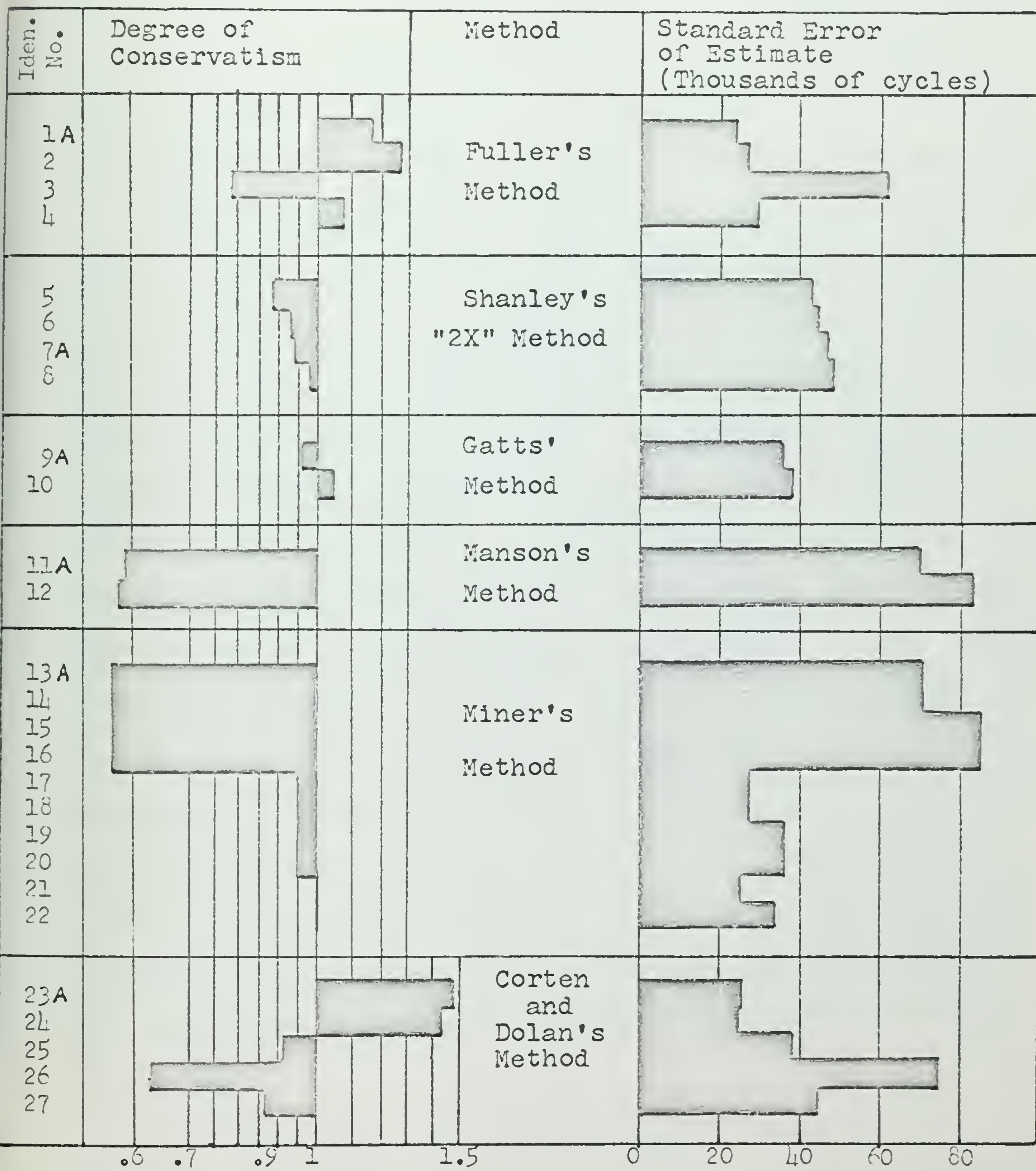

VI. DISCUSSION OF RESULTS

1. S-N Curve

The results of an analysis of constant load range data play an important role in any evaluation of proposed methods of fatigue life prediction because all proposed methods require correct representation of the allowable S-N data. The representations of the S-N curve most favored by investigators of low-cycle fatigue are the linear log S-log N and linear S-log N curves, with neither form having a clear majority. The results of this study demonstrate why opinion on the subject is divided. The linear correlation coefficients for both forms of representation are high. The semi-log representation is nearer perfect correlation (r=1.0) and has a slightly smaller error of estimate. A consideration of only the numerical values of these measures of correlation would indicate that the S-log N representation is the better. On the other hand, consideration of the fact that the fatigue damage process in metal is a statistically random process would indicate that the differences demonstrated by the constant load range tests in this study were not large enough to identify correctly the best representation. Accordingly, the close correlation of both representations required that the fatigue 1 life prediction methods be evaluated with both forms of the S-N curve.

It is known that HY-80 steel, unlike aluminum, has an endurance limit stress, S_e, but the extensive tests required

to establish the value of S_e were beyond the scope of this study. Therefore, an approximate value of the S_e for notched HY-80 steel was used, chosen by graphical methods and comparisons with similar materials. Even though the estimated value of S_e might not be the correct value, the use of an approximate value demonstrates the influence of S_e on the accuracy of the various life prediction methods.

2. Fatigue Life Prediction Methods

The statistical nature of the many facets of low-cycle fatigue damage precludes evaluating the methods for an accurate description of the fatigue damage process between damage initiation and failure. However, overall evaluations of the practical engineering value of the methods can be accomplished by analyzing and comparing the failure predictions of the various methods. The determination of the correlation of predicted fatigue life with test life provides an indication of each prediction method's reliability and adequacy.

Two measures of correlation (standard error of estimate, ϵ , and degree of conservatism, $\triangle$) are used in this study. ϵ has properties analogous to those of the standard deviation, and, as such, represents the magnitude of the deviation of the prediction from the actual values, without indicating whether the prediction is larger or smaller than the actual value. On the other hand, $\triangle$ indicates not only the scatter of the predictions, but also whether the predictions are larger or smaller than the actual values.

When using ϵ as a measure of the reliability of a prediction method, it must be remembered that the methods use the equation of the S-N curve as an entering argument. The S-N curves do not have perfect correlation and consequently reflect an ϵ of their own. Thus a value of a fatigue life prediction from a method based on the S-N curve will necessarily have an larger than that of the S-N curve.

A few observations of the effects of varying parameters may be made by noting the smallest ϵ and the $\triangle$ nearest unity in each category of each method. These six best combinations for each type of spectra provide a general indication of the effect of the parameters. In the five-level spectra, the S-log N representation yields the smallest ϵ. A change of curve forms shows no notable difference in ϵ for the 28-level spectra results. The results for all spectra show the best $\triangle$ with the S-log N curve form, but no significant difference in ϵ is produced by changing curve representations. The evaluations of the five-level, 28-level, and all stress spectra, based on S_e=0, show no conclusive difference in ϵ from those based on S_e=17,000. The results for all spectra based on S_e=0 show a slightly better $\triangle$. Thus a general consideration of $\triangle$ indicates that the S-log N curve with no S_e is the best S-N representation, while a consideration of ϵ provides no indication of the best form.

If the results of evaluating the methods as the authors proposed are ranked in order of increasing ϵ, the following order is obtained:

5-level Spectra	28-level Spectra	All Spectra
1. Corten and Dolan	1. Gatts	1. Fuller
2. Fuller	2. Shanley's "2X"	2. Corten and Dolan
3. Gatts	3. Fuller	3. Gatts
4. Shanley's "2X"	4. Corten and Dolan	4. Shanley's "2X"
5. Miner	5. Manson	5. Manson
6. Manson	6. Miner	6. Miner

When the evaluations of the authors' unmodified methods are ranked in order of increasing $\triangle$ (from unity), the order is as follows:

All Spectra

1. Gatts
2. Shanley's "2X"
3. Fuller
4. Corten and Dolan
5. Manson
6. Miner

From both the ϵ and $\triangle$ standpoint, the evaluation of the authors' unmodified methods indicates that the methods of Gatts and Fuller are best.

To understand more fully the influence of the variable parameters involved in these methods, it is necessary to considereboth the results and the formulation of each method. A brief discussion of the effect of variations on each method is given in the following paragraphs.

Corten and Dolan's Method

Although Corten and Dolan do not specify a form for the S-N curve, investigators to date have tended to use the log S-log N curve. When this representation is used for the type loadings considered in this study, δ must be lowered to improve both ϵ and $\triangle$. The results of doing so in this study do not confirm the estimates of δ cited in Appendix D. Figure IV shows the effect on ϵ and $\triangle$ when δ is varied.

Using the S-log N form of fatigue data and equating δ to the reciprocal of the slope of the curve gives a reasonable ϵ with a large $\triangle$. Increasing δ above the reciprocal of the slope (S-log N) decreases $\triangle$ but increases ϵ. This is also shown in Figure IV. The inclusion of a non-zero value for S_e improves the predictions slightly.

In order to use this method effectively, testing and iterative procedures must be used to determine the best value of δ, regardless of the S-N representation. Such a requirement severely limits the method's practical application.

Fuller's Method

Fuller's method was developed from an empirical analysis of fatigue data represented by S-log N curves with no endurance limit. Thus the method should yield the best results when the fatigue characteristics correspond to Fuller's criteria. The results of this study conform to such an expectation. All variations from the basic criteria of the author produce less accurate results.

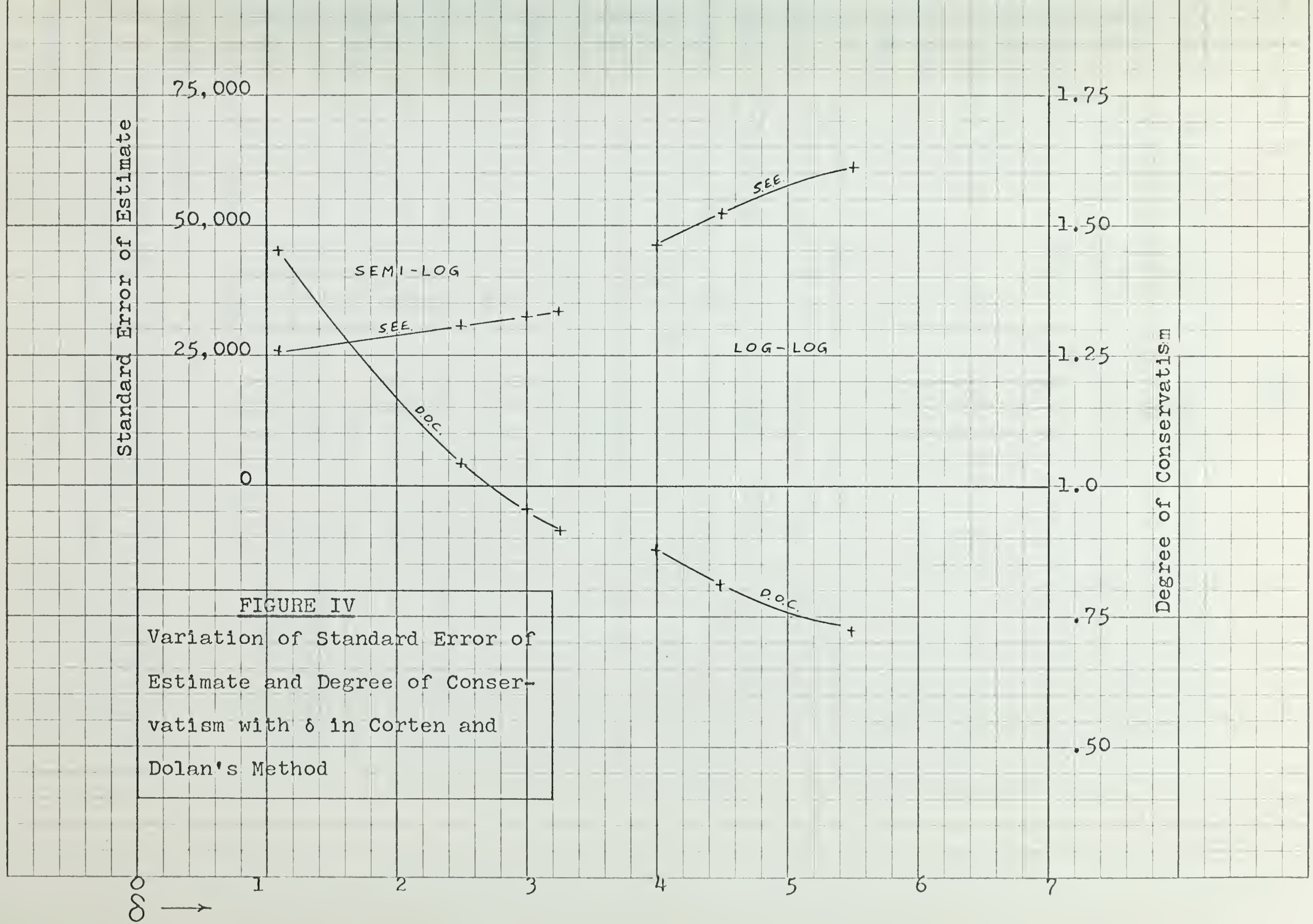

FIGURE IV

Variation of Standard Error of Estimate and Degree of Conservatism with δ in Corten and Dolan's Method

It should be noted that ϵ remained insensitive to a change in the number of stress levels in the load spectra. This is the only method that did not demonstrate a large difference of ϵ between the 28- and five-level spectra.

Gatts' Method

The evaluations of Gatts' method showed only a slight difference in results when the form of the S-N curve was changed. The Δ's for both curve forms are very near unity. The ϵ is slightly lower for the data in the S-log N curve form. The determination of the constants in this method helps explain the small difference. All the constants, except K and K', are independent of N. K and K' are determined with a value of N corresponding to an S in the loading range. The required values of N from equations (1) and (4) do not have a large difference; therefore, K and K' have no large difference.

Results obtained by this method are strongly dependent on the value used for the endurance limit stress. Predictions by this method give unreasonable results if the endurance limit stress used for calculations is not near the actual value. In fact, Gatts' method reflects a stronger dependence on the endurance limit than all the other methods considered in this study.

Manson's Method

Manson states that the applicability of his method to stresses other than cyclic bending stresses has not been verified [42]. The results of this study indicate that the

method is not applicable to stresses produced by cyclic axial loads. The predictions are very unconservative, the ϵ's are large, and the predictions reflect a strong dependence on the number of load levels. The log S-log N representation gives results with the larger error. It can be seen from equation (A 11) that the inclusion of an endurance limit increases the failure prediction and, in doing so, increases the error of the method.

An S-N curve for smooth (unnotched) HY-80 steel was not available; therefore, verification of the existence of a point of intersection, N_p, of the notched and smooth S-N curves could not be accomplished. The two extreme values for N_p (100 and 1000 cycles), as recommended by Manson, yield similar predictions, both having large errors. If N_p is assumed to be zero, the method degenerates to that of Miner. Thus, if N_p does not exist, there is no advantage in using Manson's complicated formulation to arrive at Miner's predictions. Even if N_p does exist, the method does not give reasonable predictions for axial loadings.

Miner's Method

Miner's unmodified linear damage method yields very unconservative predictions with a large ϵ. The predictions are changed very little by changing the form of the S-N curve or by giving S_e a non-zero value. The ϵ for a small number of stress levels is very much larger than the ϵ for a large number of stress levels. If the method is modified to

sum the cycle ratios, $\frac{n_i}{N_i}$, to a value other than unity, the predictions are changed. Because of the linearity of the method, using a summation of cycle ratios equal to the Δ of predictions based on a summation of unity will give new predictions having a Δ of unity. In this study, the modified summation was 0.576 for the log S-log N representation and 0.57 for the S-log N curve. These values are very close to the value of 0.6 proposed for design purposes by Pope [51]. The results obtained by using summations of 0.6, 0.57, and 0.576 are only slightly different and reduce the ϵ for a summation to unity by a factor of three.

The disparity between ϵ for the predictions for the 28-level and five-level spectra does not diminish when the summation is changed, although the ϵ's for both spectra are reasonable. In view of the ϵ of the S-N curves, the ϵ for the 28-level spectra using a modified summation is exceptionally good.

It should be noted that the ϵ and Δ remain essentially the same for the modified summations, regardless of the S-N curve form or value of S_e.

The results show that any desired Δ can be achieved by selecting the proper constant for the cycle ratio summation. For example, Miner's method will give a Δ of 1.5 if the Δ resulting from a summation to unity is divided by 1.5 and in turn used as the summation constant for a new prediction.

Shanley's "2X" Method

The use of the S-log N curve yields predictions that have lower ϵ's and are more unconservative than those obtained by using the author's specified log S-log N curve. The use of a non-zero S_e lowers the ϵ slightly and moves $\triangle$ closer to unity for both curve forms. The method is more accurate for spectra having a large number of load levels. All predictions by this method in this study are unconservative.

If the least ϵ for each method, regardless of modification, is selected, and the methods arranged in order of increasing ϵ, the following listing is produced:

Five-level Spectra

1. Corten and Dolan	unmodified
2. Fuller	unmodified
3. Miner	S-log N, $\sum$ =0.57
4. Gatts	unmodified
5. Shanley's "2X"	unmodified
6. Manson	unmodified

28-level Spectra

1. Corten and Dolan	log S-log N, δ=4.0, S_e=17,000
2. Miner	$\sum$ =0.57
3. Gatts	unmodified
4. Fuller	log S-log N, S_e=17,000
5. Shanley's "2X"	log S-log N, S_e=0
6. Manson	logS-log N, S_e=0

All Spectra

1. Miner	$\Sigma=0.57$
2. Fuller	unmodified
3. Corten and Dolan	unmodified
4. Gatts	unmodified
5. Shanley	S-log N, S_e=17,000
6. Manson	S-log N, S_e=0

Identifying the $\triangle$ closest to unity for each method, regardless of modification, and then arranging the methods in order of increasing $\triangle$ from unity gives the following:

All Spectra

1. Miner	$\Sigma=0.57$
2. Shanley's "2X"	log S-log N, S_e=0
3. Gatts	unmodified
4. Fuller	log S-log N, S_e=17,000
5. Corten and Dolan	S-log N, δ=3.25, S_e=0
6. Manson	S-log N

On the basis of the best results achieved by any method, with any modification, the method of Miner with $\Sigma=0.57$ is best. The methods of Gatts and Fuller follow Miner in best overall predictions.

It should be emphasized that, although tests of this type might bring out differences in the predictions of the various theories, the differences might not necessarily exist under other test conditions. Thus, the test conditions must closely resemble the conditions existing in the actual

structures if the degree of accuracy demonstrated by any one theory is to have practical application. Hence, these results and their implications are limited to HY-80 steel structures having a loading history similar to those used in these tests.

VII. CONCLUSIONS

1. The formulation and use of an analytically perfect fatigue damage theory must await the correct solution of the detailed stress analysis problem.

2. In the absence of definitive stress analysis, Miner's linear cumulative damage method, modified to sum the ratio, $\frac{n_i}{N_i}$, to 0.6, is the most easily applied and most accurate method currently available for the prediction of fatigue life in HY-80 steel structures.

3. Fuller's fatigue life prediction method yields reliable, though conservative, predictions whether the number of stress levels in the loading history is small or large.

4. The methods of Gatts and Shanley yield reliable life predictions only when applied to loading spectra composed of a large number of stress levels. Fatigue life predictions by Shanley's method are slightly unconservative, while those by Gatts' method show a degree of conservatism approaching unity.

5. The difficulty of determining the correct stress exponent for Corten and Dolan's method makes it impractical to apply the method to engineering problems.

6. The method of Manson evaluated in this study is not applicable to axial loadings.

VIII. RECOMMENDATIONS

1. Additional testing should be conducted to correctly define the fatigue behavior of notched HY-80 steel in the high-stress, low-life region.

2. Tests should be conducted to determine the endurance limit stress of notched, axially loaded HY-80 steel.

3. Until the stress analysis problem is solved, use Miner's linear cumulative damage method, modified to sum the ratio, $\frac{n_i}{N_i}$, to 0.6, for determining failure predictions in engineering applications.

IX. APPENDIX

A. Description of Test Apparatus

B. Description of Stress Spectra

C. Description of Fatigue Life Prediction Methods

D. Selection and Evaluation of Fatigue Life Prediction Methods

E. Mathematical Methods of Analysis

F. Bibliography

APPENDIX A

Description of Test Apparatus

The specimens for this test were manufactured from plate produced by United States Steel Corporation under Contract NObs-84479. The chemical composition of the steel is shown in Table II. The average tensile properties of the steel as obtained from duplicate 0.505-inch diameter specimens are shown in Table III. The true stress-true strain relationship of the steel is shown in Figure V.

The test specimen configuration is shown in Figure VI. The notch has a theoretical stress concentration factor of 2.75. The test section of the specimen is identical to the V-notch cantilever beam specimen used by Marine Engineering Laboratory in low-cycle flexure fatigue tests. The selection of a V-notch specimen was based on the success of the David Taylor Model Basin in correlating structural fatigue results with V-notch data.

The specimens were cycled on a Wiedemann-Baldwin, Mark 300-AL, Universal Testing Machine. This machine has the capacity of a 300,000-pound load in both tension and compression. It can be controlled automatically by load, strain, or crosshead movement. To permit automatic performance of the multilevel tests, an auxiliary control panel, shown in Figure VII, was designed and constructed at the U.S. Navy Marine Engineering Laboratory.

APPENDIX A

Description of Test Apparatus

The specimens for this test were manufactured from plate produced by United States Steel Corporation under Contract NObs-86479. The chemical composition of the steel is shown in Table II. The average tensile properties of the steel as obtained from duplicate 0.505-inch diameter specimens are shown in Table III. The true stress-true strain relationship of the steel is shown in Figure V.

The test specimen configuration is shown in Figure VI. The notch has a theoretical stress concentration factor of 2.75. The test section of the specimen is identical to the V-notch cantilever beam specimen used by Marine Engineering Laboratory in low-cycle flexure fatigue tests. The selection of a V-notch specimen was based on the success of the David Taylor Model Basin in correlating structural fatigue results with V-notch data.

The specimens were cycled on a Wiedemann-Baldwin, Mark 300-AL, Universal Testing Machine. This machine has the capacity of a 300,000-pound load in both tension and compression. It can be controlled automatically by load, strain, or cross-head movement. To permit automatic performance of the multi-level tests, an auxiliary control panel, shown in Figure VII, was designed and constructed at the U.S. Navy Marine Engineering Laboratory.

The criterion for failure was the propagation of a crack to a distance of 1/8 to 3/16 inch from the edge of the notch. This condition was detected with a loop of insulated copper wire cemented to the specimen 1/8 inch from the tips of the notch. The wire loop was part of the electrical control circuit. As the crack propagated outward from the notch, it reached the wire and caused the wire to break. The breaking of the wire stopped the machine.

TABLE II

Chemical Composition of the Steel

Element	C	Mn	P	S
Per cent	0.2	0.28	0.01	0.015
Element	Si	Ni	Cr	Mo
Per cent	0.23	3.04	1.48	0.47

TABLE III

Tensile Properties of the Steel

Property	Value
0.2 Per cent Yield Strength, psi	80,500
Tensile Strength, psi	98,000
Elongation in 2 in., per cent	29.0
Reduction in Area, per cent	76.0
True Fracture Stress, psi	175,000

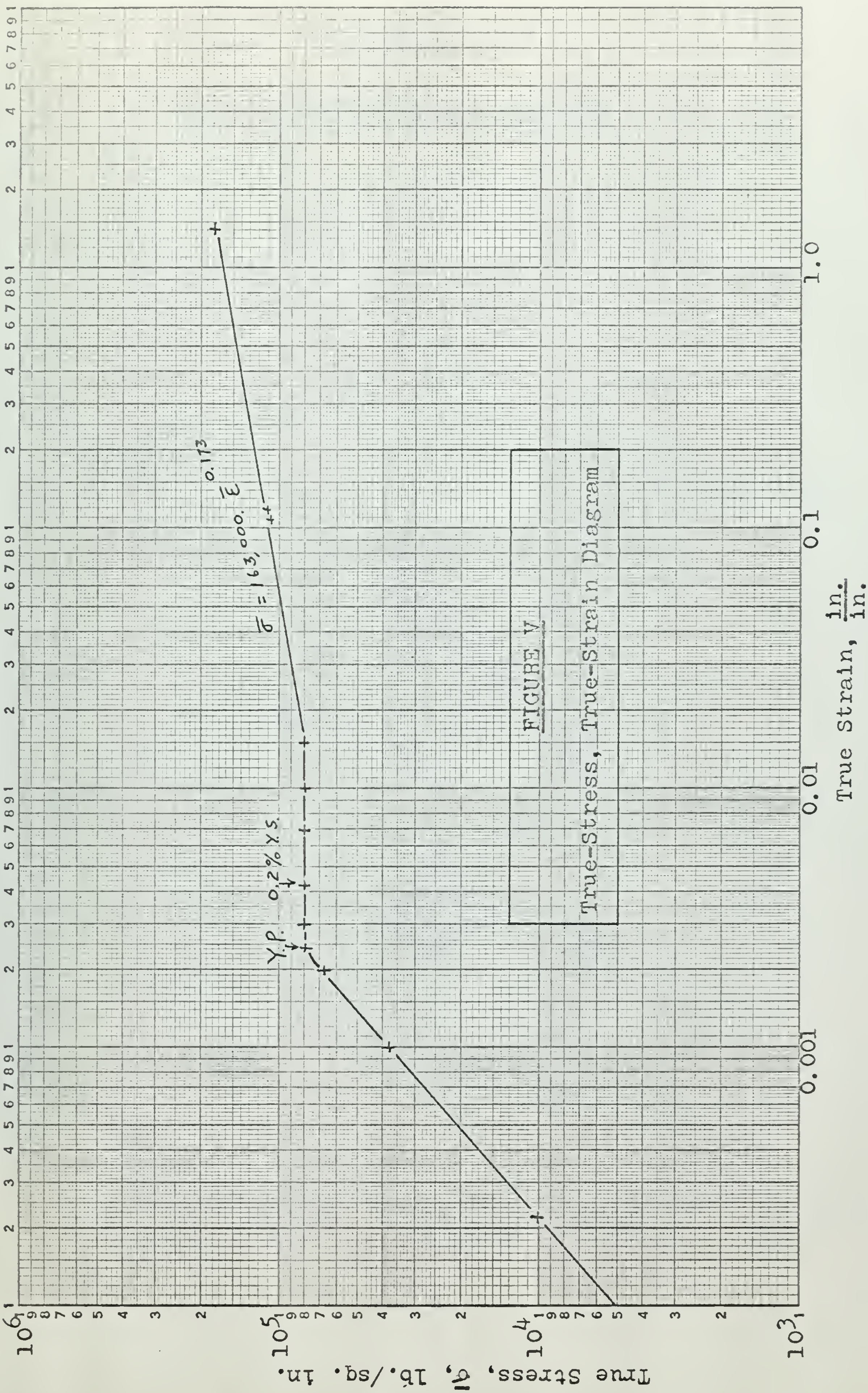

FIGURE V

True-Stress, True-Strain Diagram

FIGURE VI

AXIAL FATIGUE, V-NOTCH SPECIMEN

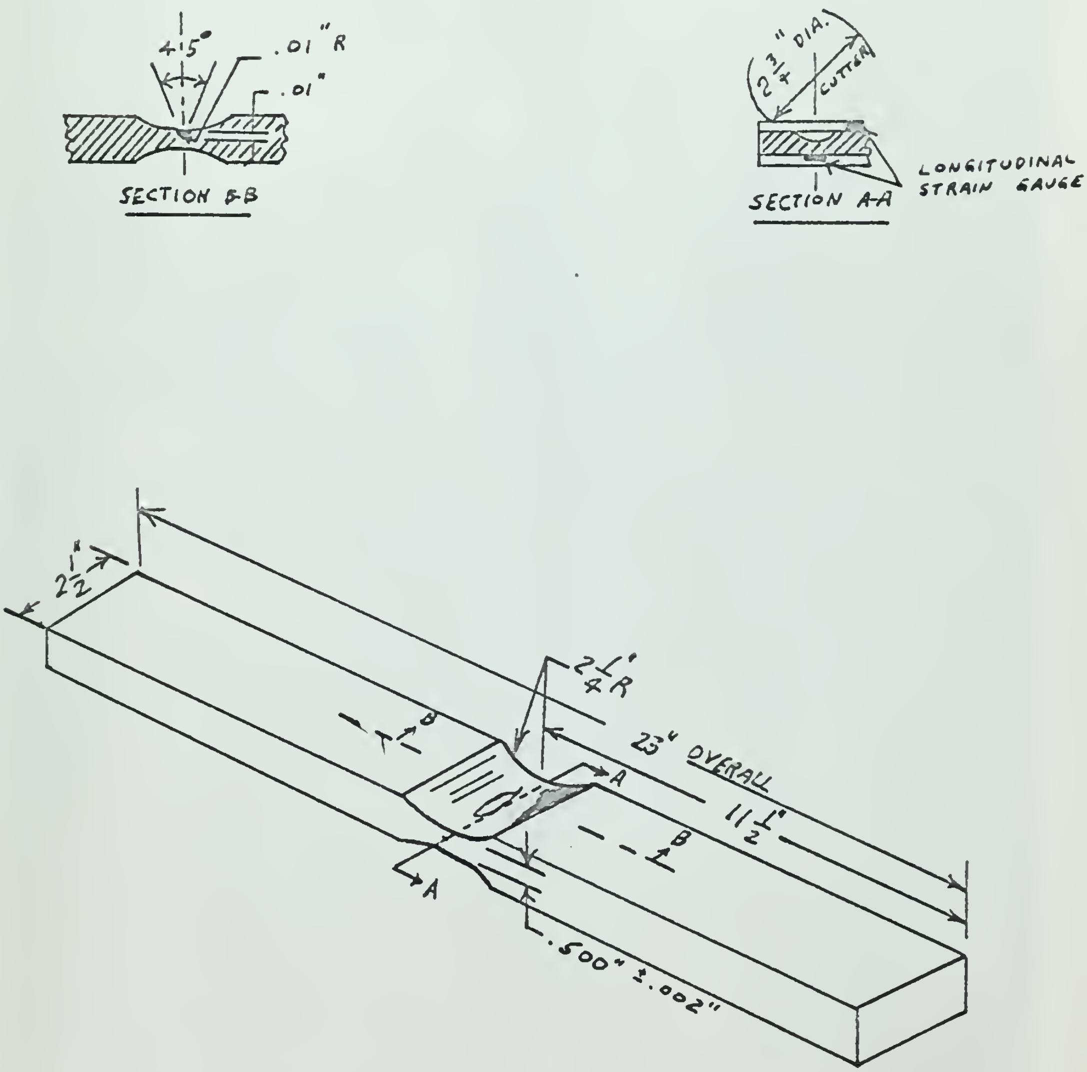

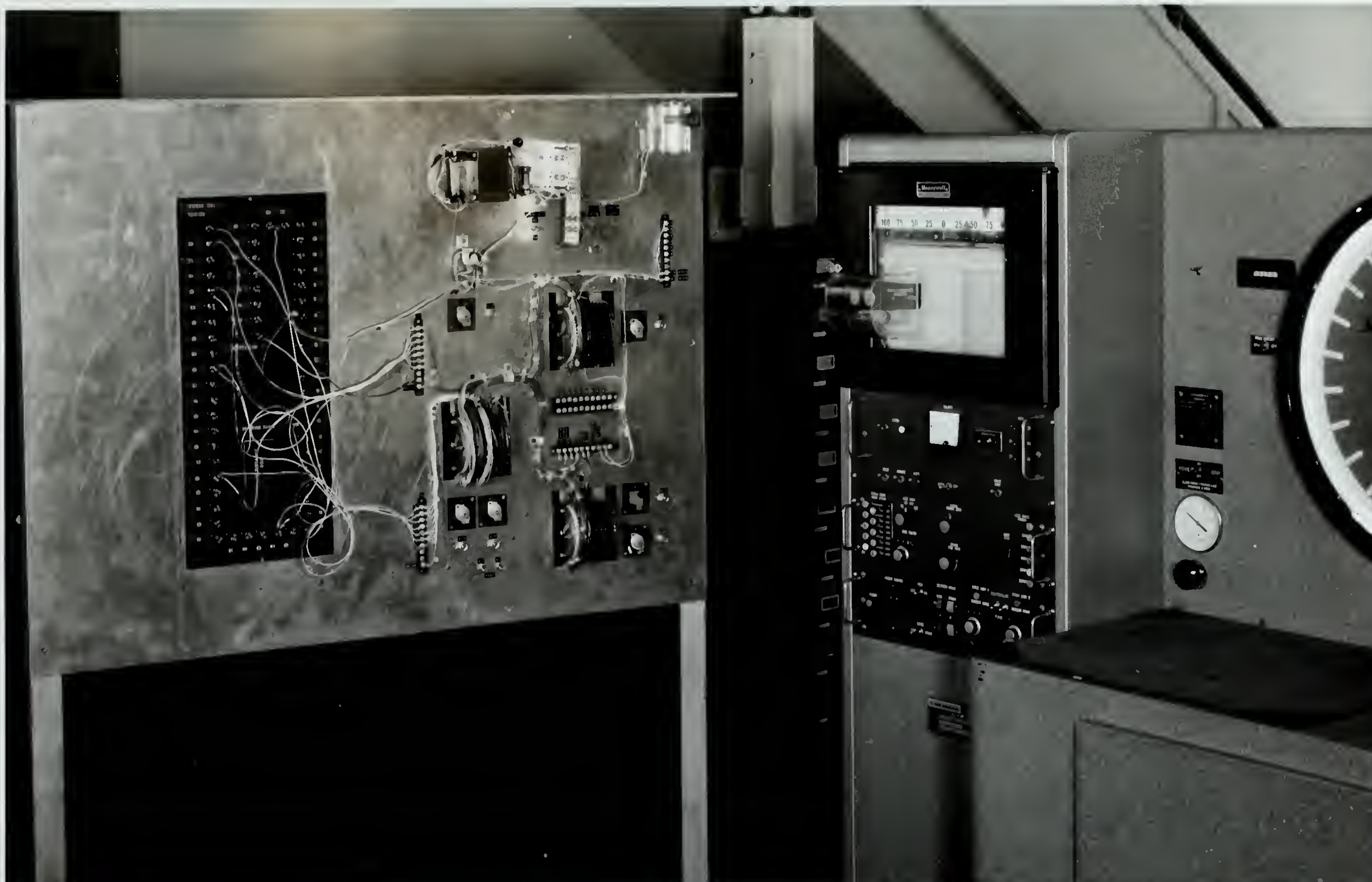

FIGURE VII

28-Level Test Program Control Panel

APPENDIX B

Description of Stress Spectra

The stress cycle combinations furnished by the Bureau of Ships were reduced to eighteen spectra. Nine of the spectra represented nine combinations of residual and working stresses with 28 different stress conditions per spectrum. The remaining nine spectra represented the same load ranges, but contained only five different stress conditions per spectrum. The maximum stress in a spectrum corresponded to a residual tensile stress of 50, 75, or 100 per cent of the minimum yield strength of HY-80 steel. Different values of compressive working stresses were combined with the maximum stress to establish various stress conditions within the load range of the spectrum. Each stress condition within a spectrum was assigned a frequency of occurrence on the basis of loading histories of actual structures. Figure VIII is a graphic illustration of a typical 28-stress level spectrum, and Figure IX shows a typical five-stress level spectrum. A complete listing and a description of the stress combinations are given in reference [57].

The nine load ranges of the spectra were used for the constant load-range tests. In addition, four completely reversed stress tests were performed to define more accurately the low and high life portions of the S-N curve.

Each of the variable load-range tests conformed to one of

the eighteen spectra of 28 or five levels. A 28-level spectra was not tested if its corresponding constant load-range test did not produce failure. The load spectrum was continuously repeated until failure occurred or 100,000 cycles were reached.

The calculations for developing the stress levels in the specimen were based on the initial cross-sectional area at the minimum section of the specimen, exclusive of notch effects.

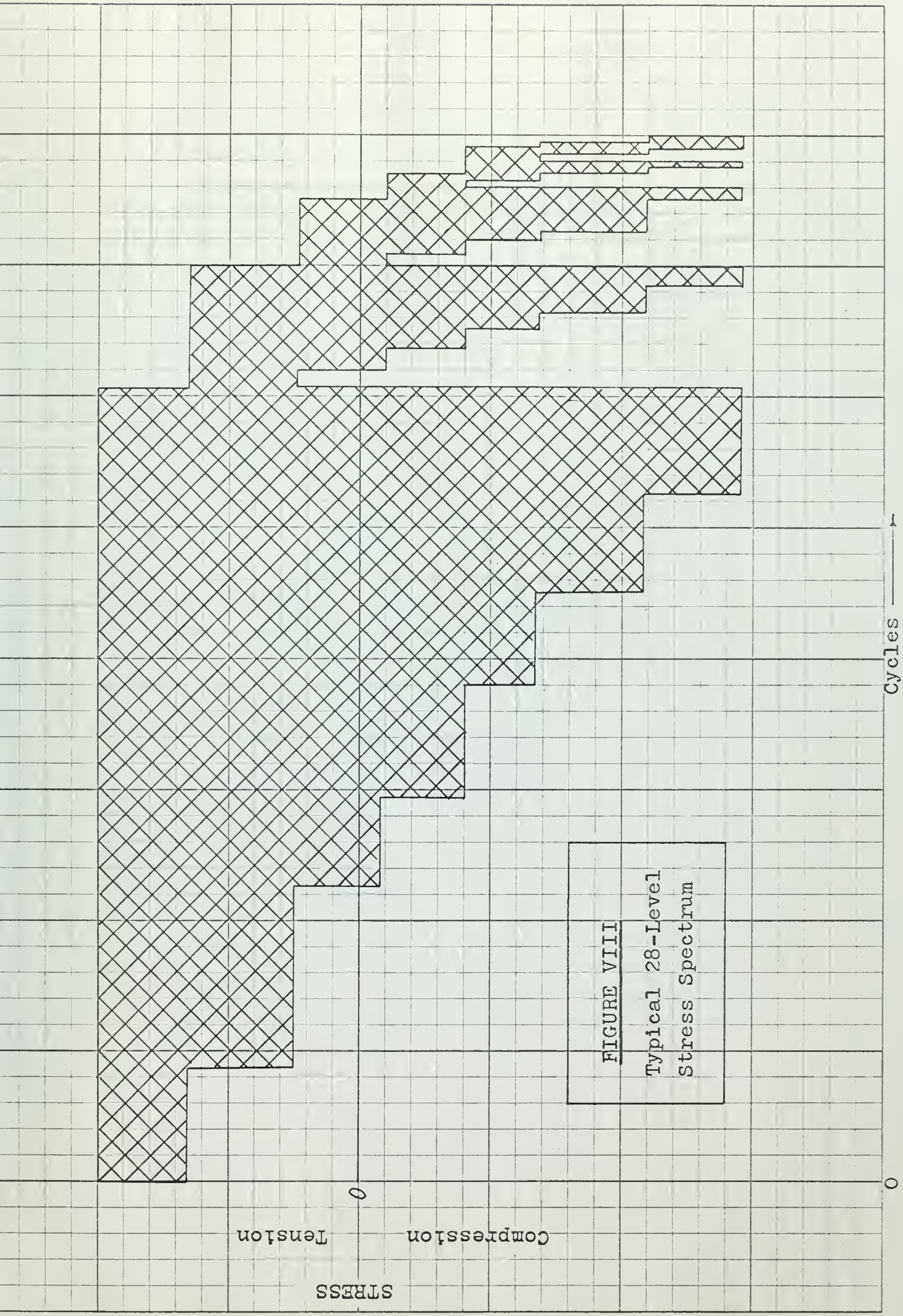

FIGURE VIII

Typical 28-Level Stress Spectrum

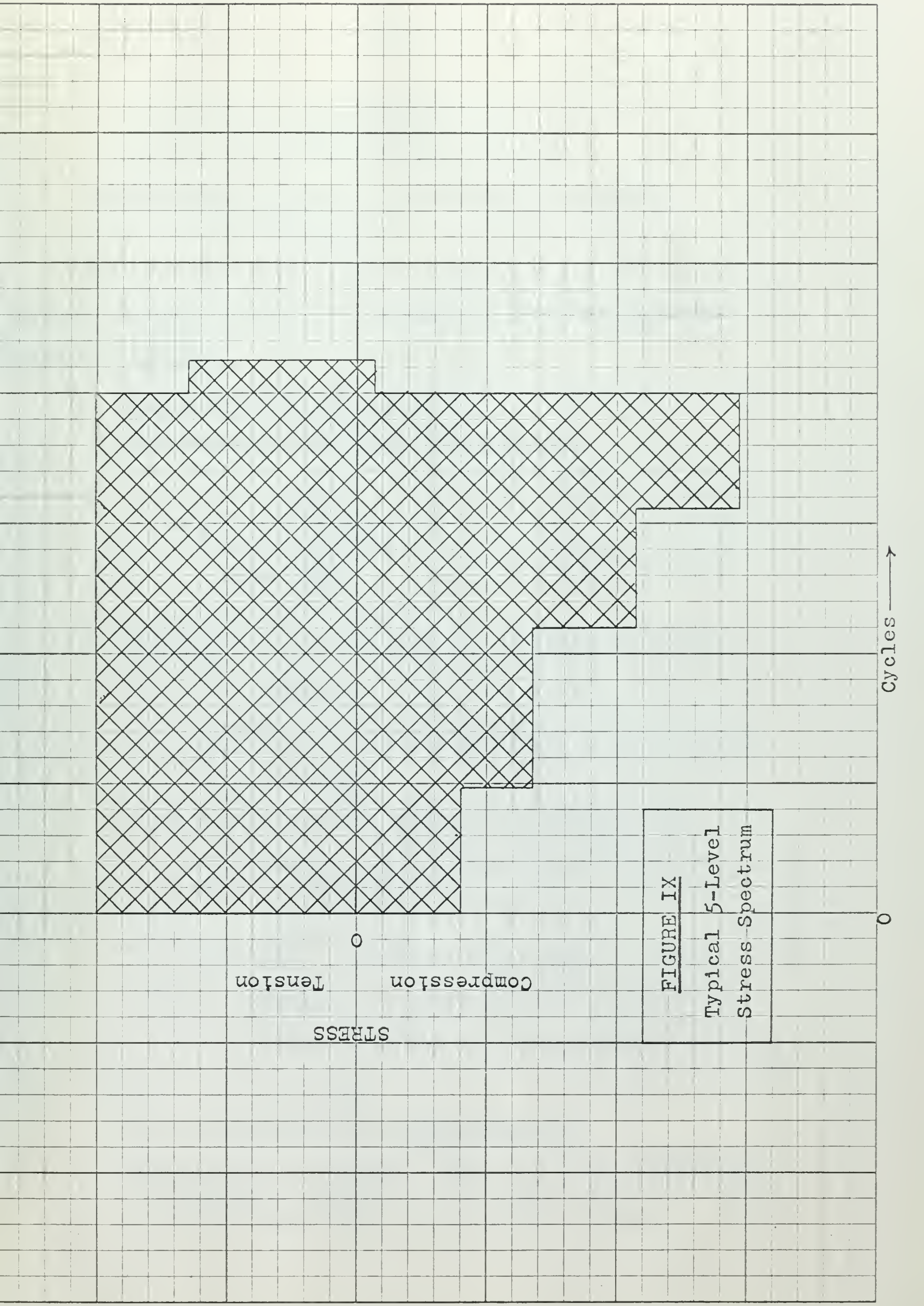

FIGURE IX

Typical 5-Level Stress Spectrum

APPENDIX C

Description of Fatigue Life Prediction Methods

This appendix describes the procedure for utilizing the various methods to predict the life of material subjected to low-cycle fatigue.

1. Corten and Dolan's Method [6]

The following equation is evaluated:

$$N_f = \frac{N_z}{\sum \left(\alpha_i \left[\frac{S_i}{S_z} \right]^{\delta} \right)} \tag{A 1}$$

where N_f = predicted number of cycles to fatigue failure

S_z = largest stress amplitude in the loading spectrum

N_z = number of cycles to failure at S_z

S_i = stress amplitude at the i^{th} varying load in the spectrum

$\alpha_i = \frac{n_i}{\sum n_i}$ = ratio of the number of cycles applied at S_i to the total number of cycles applied in the normalized loading sequence

δ = invariant stress exponent

All stresses, including those below the endurance limit, are considered to contribute damage.

2. <u>Freudenthal and Heller's Method</u> [14]

Cycles to failure are predicted by

$$N_f = \frac{1}{\sum \left[\frac{n_i \ \omega_i}{N_i} \right]} \tag{A 2}$$

where n_i = number of cycles applied at the i^{th} varying stress, S_i

N_i = number of cycles to failure at the i^{th} varying stress, S_i

ω_i = a stress interaction factor which reduces the number of cycles to failure at the i^{th} level to account for prior higher stresses

3. <u>Fuller's Method</u> [16]

The stresses within a block of stress levels which has many repetitions are arranged in descending order without regard for their actual order of occurrence. The stresses are normalized to a 1000-cycle block and plotted on a three-cycle semi-logarithmic plot, as shown in Figure X. The distribution coefficient, β, is defined as the ratio of the shaded area in Figure X to the total area bounded by $N = 1$, S_z (the highest applied stress level), $N = 1000$, and S_a (the smallest applied stress level).

N_f is found from the equation

$$N_f = N_a \left[\frac{N_z}{N_a} \right]^{\beta} \tag{A 3}$$

FIGURE X

Determination of β for Fuller's Method

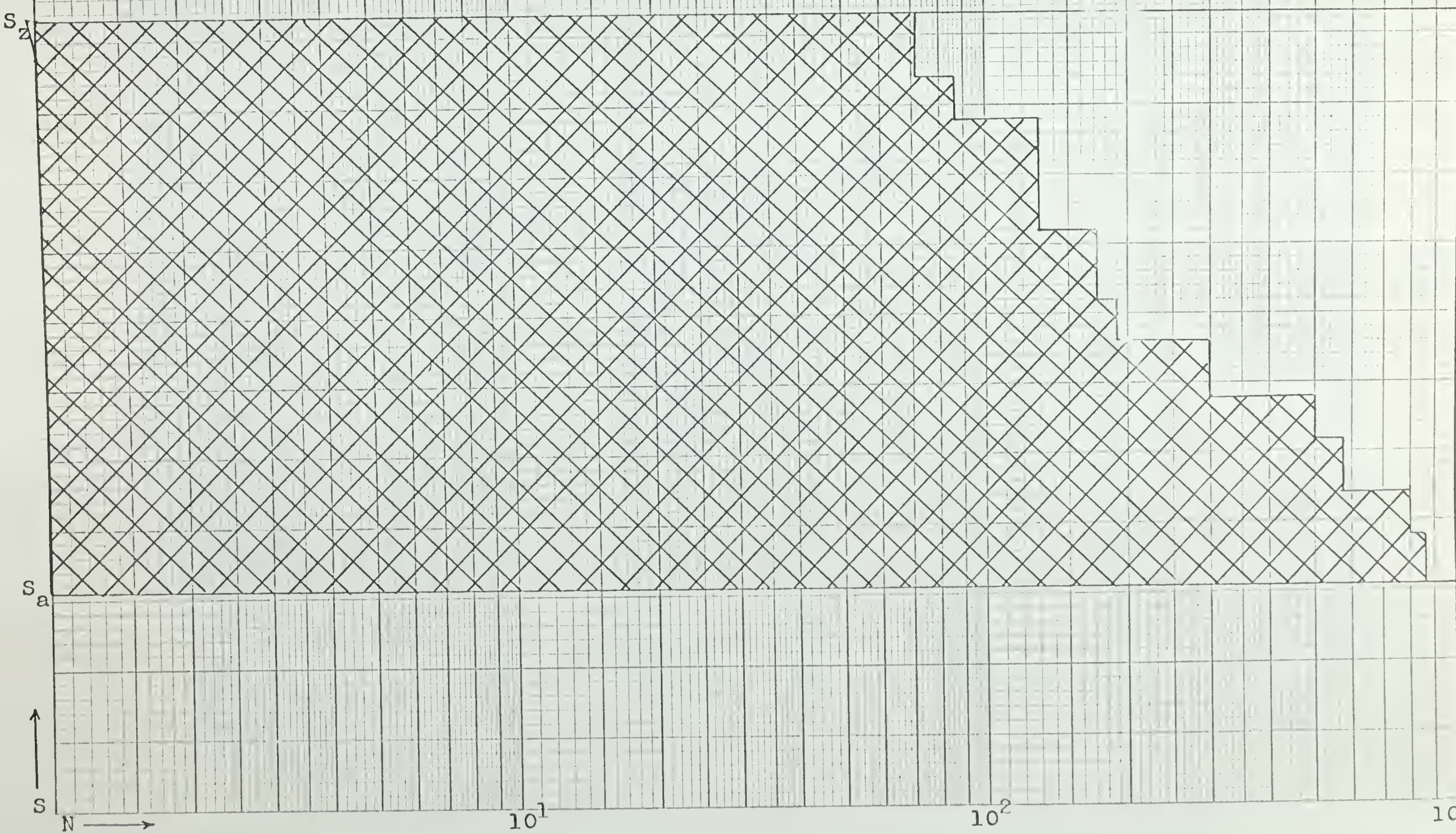

where N_a = the number of cycles to failure at S_a

N_z and N_a are taken from the straight line, $S - \log N$ curve linearly extended to S_a.

4. <u>Gatts' Method</u> [17]

Assign each stress amplitude, S_i, a probability, ρ_i; for example, on the average in 100 cycles, S_1 will occur $\rho_1 \times 100$, etc.

Define λ as the ratio of the endurance limit of the virgin material, S_{eo}, to the ultimate tensile stress, S_{fo}, i.e.

$$\lambda = \frac{S_{eo}}{S_{fo}}$$

For a known value of N for a particular S, evaluate K from the relation

$$KN = \left[\frac{1}{S - S_{eo}}\right] - \left[\frac{1}{S(1-\lambda)}\right]$$

Determine values for the constants, K', c, and b, from

$$K' = K\sum \rho_i$$

$$c = \frac{\sum \rho_i S_i^{\,2}}{\sum \rho_i}$$

$$b = \frac{\sum \rho_i S_i}{\sum \rho_i}$$

For discrete values of stress amplitude, the constants include only the sums for those values of i for which S_i is greater than S_e.

Determine N_f from

$$K'N_f = \frac{1}{\sqrt{c-b^2}}\left\{\tan^{-1}\left\{\frac{(b-\lambda S_z)}{\sqrt{c-b^2}}\right\}-\tan^{-1}\left\{\frac{(b-S_{eo})}{\sqrt{c-b^2}}\right\}\right\} \quad (A\ 4)$$

5. Henry's Method [27]

Define the S-N characteristics of the material in the form

$$N = \frac{C}{S_i - S_{eo}}$$

Fatigue damage at any stress greater than S_{eo}, but less than 1.5 S_{eo}, is represented by

$$D = \frac{\frac{n_i}{N_i}}{1+\frac{S_{eo}}{(S_i-S_{eo})}\left[1-\frac{n_i}{N_i}\right]}$$

For several discrete load levels above the endurance limit,

$$D_i = \frac{\left(\frac{n}{N}\right)_{i-1}+\frac{n_i}{N_i}}{1+\frac{S_{eo}}{(S_i-S_{eo})}\left[1-\left(\frac{n}{N}\right)_{i-1}+\left(\frac{n_i}{N_i}\right)\right]} \quad (A\ 5)$$

where D_i = damage ratio after applying cycles at the i^{th} level

$\left(\frac{n}{N}\right)_{i-1}$ = equivalent cycle ratio at the $(i-1)^{th}$ level

Repeated use of equation (A 5) will give the fatigue damage of a sequence of load levels.

Predict N_f from

$$N_f = \frac{\sum n_i}{\sum D_i} \qquad (A\ 6)$$

6. Langer's and Grover's Methods [21,33]

The equations to be satisfied are

$$\sum \frac{\mu_i}{\gamma_i N_i} = 1 \quad \text{and} \quad \sum \frac{x_i}{N_i(1-\gamma_i)} = 1$$

where μ_i = the number of load cycles applied before crack initiation

γ_i = the per cent of the number of cycles to failure required to initiate cracks at the i^{th} load level

x_i = the number of load cycles applied between crack initiation and final failure

Thus the number of cycles to failure for a specific stress level is

$$(N_f)_i = (\mu_i + x_i) \qquad (A\ 7)$$

7. Levy's Method [35]

For two-step loading (assuming that less than one application of the higher load level in 10,000 total load cycles will have no effect on the S-N curve at the lower stress level), the following equation is applied

$$N_f = \sqrt{\left[N_2^{\log\left(\frac{10000n_2}{n_1+n_2}\right)}\right] N_1^{\log\left(\frac{n_1+n_2}{n_2}\right)}}$$

For more than two loading steps, the following equation is evaluated:

$$\log N_f = a' \log \frac{n_1}{n_i} + b' \log \frac{n_2}{n_i} + \ldots + M \quad \text{(A 9)}$$

where a', b', . . . , etc. are constants reflecting the values of N_1, N_2, . . . , N_i and M is a constant coefficient of the loading spectrum.

8. Lundberg's FFA Method [39]

The S-N curve of the material is represented in the form

$$N = \frac{A}{\left[S_i - S_e\right]^{B}}$$

where A = the value of S_i for N = 1 from the straight line plot of log $(S_i - S_e)$ versus log N

B = the slope of the straight line fit of log $(S_i - S_e)$ versus log N

A cumulative unit loading spectrum is drawn by plotting S_i versus log J, where J is the total number of cycles applied at or above S_i.

The damage ratio, D_L, for the unit distribution is

$$D_L = \frac{J_o}{A} j^{-B} e^{(-jS_e)} \Gamma(B+1)$$

where J_o = intercept at S_i=0 of the straight line fit to the unit loading spectrum on S_i-log J coordinates

j = slope of the straight line fit to the unit loading spectrum on S_i-log J coordinates

$\Gamma(B+1)$ = Gamma function of (B+1)

Apply the following for a life prediction:

$$N_f = \frac{\sum n_i}{D_L} \qquad \text{(A 10)}$$

9. Manson's Method [42]

The following equation is applied:

$$\frac{n_{r,i+1}}{N_{i+1}} = \left\{\left(\left[\left(1-\frac{n_1}{N_1}\right)^{\frac{\log\frac{N_2}{N_p}}{\log\frac{N_1}{N_p}}} - \frac{n_2}{N_2}\right]^{\frac{\log\frac{N_3}{N_p}}{\log\frac{N_2}{N_p}}} - \frac{n_3}{N_3}\right)^{\frac{\log\frac{N_4}{N_p}}{\log\frac{N_3}{N_p}}} \cdots\cdots \cdots\cdots - \frac{n_i}{N_i}\right\}^{\frac{\log\left(\frac{N_{i+1}}{N_p}\right)}{\log\frac{N_i}{N_p}}} \qquad \text{(A11)}$$

where $n_{r,i+1}$ = number of cycles of life remaining after i number of pre-stresses (that is, number of cycles of life remaining at the (i+1) stress level)

N_{i+1} = number of cycles to failure at the (i+1) stress level, according to the original material S-log N curve

N_p = the number of cycles to failure at the intersection of the S-log N lines as established by tests, or an estimated value between 100 and 1000 cycles

Failure is predicted when the product of N_{i+1} and the right side of (A 11) is equal to or less than the number of cycles applied at the i+1 level. Designating the failure level as $(n_{f,i+1})$, the total cycles to failure are

$$N_f = \sum n_i + (n_{f,i+1}) \qquad \text{(A 12)}$$

10. Miner's Method [45]

For each value of S_i, determine the corresponding N_i. Form the ratio $\frac{n_i}{N_i}$ for each S_i and evaluate the following:

$$N_f = \frac{1}{\sum\left(\frac{n_i}{N_i}\right)} \qquad \text{(A 13)}$$

11. Methods of Richart and Newmark [53] and Marco and Starkey [43]

Develop damage curves as a function of both the load level and cycle ratio $\left(\frac{n_i}{N_i}\right)$. Each curve must indicate a damage level of unity when the cycle ratio is unity. By the method of Richart and Newmark, the damage curves may be described relative to an arbitrary damage curve at any reference load level. By the method of Marco and Starkey, the shape of the load curve at each load amplitude may be made a function of the cycle ratio raised to a stress-dependent exponent, Ω; i.e.

$$D_i = \left(\frac{n_i}{N_i}\right)^{\Omega}$$

Once D_i has been adequately defined, N_f can be determined with equation (A 6).

Failure is predicted when the product of n_{i+1} and the right side of (4.11) is equal to or less than the number of cycles applied at the i+1 level. Designating the failure level as $(n_{i,i+1})$, the total cycles to failure are now:

$$N_f = \sum n_i + (n_{i,i+1}) \qquad (4.12)$$

10. Miner's Method [45]

For each value of S_i, determine the corresponding N_i. Form the ratio $\frac{n_i}{N_i}$ for each S_i and evaluate the following:

$$N_f = \frac{1}{\sum\left(\frac{n_i}{N_i}\right)} \qquad (4.13)$$

11. Methods of Richart and Newmark [51] and Marco and Starkey [43]

Develop damage curves as a function of both the load level and cycle ratio $\left(\frac{n_i}{N_i}\right)$. Each curve must indicate a damage level of unity when the cycle ratio is unity. In the method of Richart and Newmark, the damage curves may be described relative to an arbitrary damage curve at any reference load level. In the method of Marco and Starkey, the shape of the load curve at each load amplitude may be made a function of the cycle ratio raised to a stress-dependent exponent, $\Omega \geq 1.0$.

$$D_i = \left(\frac{n_i}{N_i}\right)^{\Omega}$$

Once D_i has been adequately defined, N_f can be determined with equation (2.5).

12. Shanley's "1X" and "2X" Methods [58,59,60]

(a) "1X"

Represent S-N data in the form

$$N = \frac{C_s}{S^d}$$

Solve for S_R, the reduced stress of constant amplitude,

$$S_R = \left(\frac{\sum n_i S_i{}^d}{\sum N_i} \right)^{\frac{1}{d}}_{S_i > S_e}$$

N_R, the total number of cycles that may be applied at all load levels above the endurance limit prior to failure, is found from

$$S_R = \left(\frac{C_s}{N_R} \right)^{\frac{1}{d}}$$

For a loading sequence which includes stresses below the endurance limit, the predicted cycles to failure are

$$N_f = N_R + (\sum n_i)_{S_i < S_e} \qquad \text{(A 14)}$$

(b) "2X"

Evaluate

$$N_f = \left\{ \sqrt{\frac{(\sum n_i)_{S_i > S_e}}{\sum \left(\frac{n_i}{N_i^2} \right)}} \right\} \frac{(\sum n_i)_{\text{unit block}}}{(\sum n_i)_{S_i > S_e}} \qquad \text{(A 15)}$$

13. Smith's Method [61]

Evaluate the actual stress, S_T, (residual plus

external) at each load level. Determine a N_i for each $(S_T)_i$ from the unnotched S-N curve of the material and apply equation (A 13).

14. Valluri's Method [62,62]

Solve equation (A 16) simultaneously at two values of N_i in the same region of the basic S-N curve to determine the constants τ and K_v

$$N_i = \frac{\tau \ln\left[\frac{S_{fo}}{S_i}\right]^{a_t} \ln\left[\frac{S_i - S_e}{K_v}\right]}{\left[\frac{S_i - S_e}{E}\right]^2 \left[\frac{S_i}{S_e}\right]^2} \qquad \text{(A 16)}$$

where $a_t \cong 2$ for brittle materials

$a_t \cong 5$ for ductile materials

τ and K_v vary over the entire region of the curve and must be determined over the entire range of the applied stress. Equation (A 17) is solved at each applied stress level and plotted versus $\ln N_i$. (See Figure XI).

$$\ln\frac{l}{l_o} = \frac{\left[\frac{S_i - S_e}{E}\right]^2 \left[\frac{S_i}{S_e}\right]^2 (2N_i)}{\tau \ln\left[\frac{S_i - S_e}{K_v}\right]} \qquad \text{(A 17)}$$

where $\frac{l}{l_o}$ = crack length ratio

Each curve shows the progress of the crack length during a fatigue test in which the stress amplitude and

range are maintained constant. For the actual use of the curves, the basic reference should be consulted.

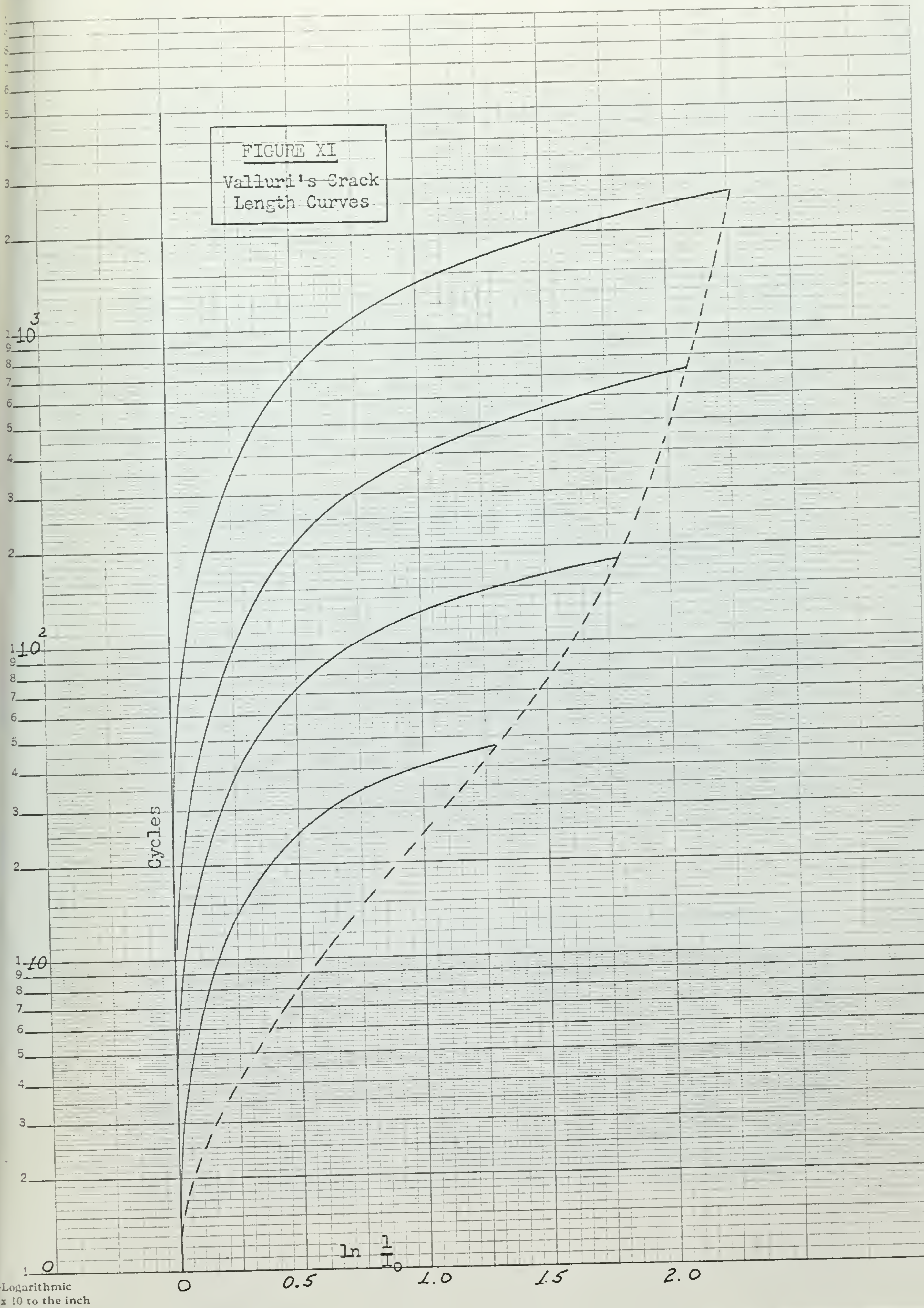
FIGURE XI
Valluri's Crack Length Curves
Cycles
10^3
10^2
10
0
$\ln \frac{l}{l_0}$
0
0.5
1.0
1.5
2.0
Semi-Logarithmic
cycles x 10 to the inch

APPENDIX D

Selection and Evaluation of Fatigue Life Prediction Methods

From the sixteen fatigue life prediction methods selected for comparative study, six methods were chosen for comparison by numerical evaluation. The limitations which precluded the numerical evaluation of the remaining ten methods are discussed below.

1. Freudenthal and Heller's Method

Lack of the type of data required to determine the stress interaction factor, ω_1, prevented the application of this method. As indicated in Section II, a large number of tests are required to derive ω_1. Freudenthal and Heller indicate that although the dependence of ω_1 on the load spectrum has been established, the exact relationship governing stress interaction phenomena is not yet known [26].

2. Henry's Method

The limitation on applicability of this method to those cases where the applied stresses are less than or equal to 1.5 times the endurance limit stress, S_{eo}, prevented the use of the method. Although the exact value of S_{eo} for the HY-80 steel used in these tests was not known, a reasonable estimate for the material in the notched condition would be 17,000 psi. The maximum

APPENDIX D

Selection and Evaluation of Fatigue Life Prediction Methods

From the sixteen fatigue life prediction methods selected for comparative study, six methods were chosen for comparison by numerical evaluation. The limitations which precluded the numerical evaluation of the remaining ten methods are discussed below.

1. Freudenthal and Heller's Method

Lack of the type of data required to determine the stress interaction factor, ω_1, prevented the application of this method. As indicated in Section II, a large number of tests are required to derive ω_1. Freudenthal and Heller indicate that although the dependence of ω_1 on the load spectrum has been established, the exact relationship governing stress interaction phenomena is not yet known [26].

2. Henry's Method

The limitation on applicability of this method to those cases where the applied stresses are less than or equal to 1.5 times the endurance limit stress, S_{eo}, prevented the use of the method. Although the exact value of S_{eo} for the HY-80 steel used in these tests was not known, a reasonable estimate for the material in the notched condition would be 17,000 psi. The maximum equivalent reversed stresses in the loading spectra were considerably in excess of 1.5 times the estimated S_{eo}. It should be noted that this method accounts for both the effect of stress block size and the order of load application. Evaluation becomes very complex when more than two load levels are considered. If S_{eo} is assumed to be zero, Miner's method results.

3. Langer's and Grover's Methods

Data providing the number of cycles to crack initiation and the additional number of cycles to failure in HY-80 steel were not available for these tests. If the phenomena of crack initiation and propagation are shown to be linear, these methods should give valid failure predictions. If the curves for crack initiation and for failure are found to be parallel, these methods will reduce to the simple linear cumulative damage relation. At the present time, the accurate determination of crack initiation prevents the application of these methods to practical engineering problems.

4. Levy's Method

Six sets of five stress-level data were available to solve simultaneously for the (q+1), i.e. six, constants required by Levy's method for five-stage data; however, no data would have been available for analysis after the constants were evaluated. There were not enough test sets to evaluate the constants for the 28-stage loading

spectra. If there had been sufficient data in both cases, only one equation per spectrum would have been necessary to predict the fatigue life of each unit spectrum.

5. Lundberg's FFA Method

An attempt was made to define the loading spectra with curves of the analytical form required by this method. The shape of the unit loading spectra could not be adequately defined by a straight line fit in the stress range of maximum fatigue damage. Since the results of this method are highly dependent on a good fit of the curves, the method was not numerically evaluated.

6. Methods of Richart and Newmark and Marco and Starkey

To apply these methods to test results, special two-step loading test data is required in large quantities to define the relationship between damage boundaries. This experimental data was not available for HY-80 steel.

7. Shanley's "1X" Method

The S-N data of the material used in this study was described in a form that reduced this approach to the method of Miner. The numerical results obtained by Miner's method represent those that would be obtained by Shanley's "1X" procedure.

8. Smith's Method

This method requires the solution of a complex stress analysis problem before it can be applied. Since detailed stress analysis was not the objective of this in-

vestigation, the residual internal stresses after each stress loading were not evaluated. Previous use of this method has been limited to simple two-step loading sequences on simple coupons, and the extension of the method to five- or 28-step loading sequences was not undertaken in this study.

9. Valluri's Method

The constants τ and K_v could not be determined with sufficient accuracy for use in this evaluation. Previous investigations indicate that this method does not give realistic estimates for program loading of the type to which the specimens in this test were subjected [63]. When applied, this method requires lengthy calculations and plotting procedures which do not lend themselves to computerization. Although Valluri does not account for all parameters in a way that satisfies all investigators, he presents a method that appears to be the first attempt to introduce the proper sequence of events into a single relation. The implications of this method are not in all cases in agreement with experimental evidence. For example, in a two-stress level test, the method implies that a greater life will be obtained if the high stresses are applied first.

Each of the six methods chosen for numerical comparison was evaluated with the test data following the procedure spe-

cified by the proposing author. As noted in Appendix C, each of these methods reflected variations in handling certain aspects of the problem, such as the representation of the load spectra, the equation of the S-N curve, or the existence of an endurance limit. In this study, additional variations were applied. After the methods had been numerically evaluated by the procedure proposed in the literature, the methods were modified and extended so that predictions reflecting a linear log S-log N curve, a linear S-log N curve, an endurance limit, and no endurance limit were obtained for each method.

Because no reliable endurance limit had been established for the material used in these tests, estimation procedures and comparisons with similar materials were used to establish an endurance limit for use in the tests.

Considerations other than those of S-N representation and endurance limit which governed the selection and evaluation of the six methods are given below.

1. Corten and Dolan's Method

As presented by Corten and Dolan, the stress exponent, δ, is invariant and has a value of 6.57 for a two-stress level experiment. Other investigators maintain that δ is not constant, but instead varies with material, configuration, and/or stress ratio [55]. Valid estimates of the fatigue life of built-up structures have been found using this method with δ varying from 8.25 to 10.3 [46]. Appendix II, reference [46], presents a discussion

of the variation of predicted life as a function of δ. It has also been suggested that the non-linearity of damage propagation which is considered in detail by this method appears to be of relatively minor importance in the case of notched specimens when the influence of residual stresses is present [28,54].

A consideration of the above remarks and the realization that the method reduces to Miner's method if δ is taken as the absolute value of the slope of the log S-log N curve, prompted the use of a range of values of the exponent δ when evaluating this method.

2. Fuller's Method

Predictions by this method show a strong dependence on the exponent β. In addition to the variations induced in β by S-N and S_e representations, β was altered in the five-stage tests by not normalizing the data to 1000 cycles.

3. Gatts' Method

The formulation of this method does not permit evaluation at an endurance limit of zero, nor does it give reasonable results for a small endurance limit. Accordingly, Gatts' method was not evaluated using an endurance limit of zero.

4. Manson's Method

This method was evaluated in an attempt to verify its applicability to stresses other than cyclic bending

stresses. Because no S-N curve for smooth specimens was available from which an intersection of S-N curves (N_p) could be established, the recommended limits of approximate values of N_p were used. An assumption of no intersection would have reduced the method to that of Miner.

5. Miner's Method

References [19] and [23] state that the energy assumptions on which Miner based this method are incorrect and evaluations of the method by several investigators yield results which differ from observed values. In fact, most of the other methods considered in this study represent modifications which attempt to improve the basic cumulative damage analysis. Additional modifications were applied to include evaluations for which the summation $\sum \frac{n_i}{N_i}$ was not equal to unity.

6. Shanley's "2X" Method

For some investigators this method yields predictions with a large degree of conservatism. Others criticize the method because Shanley made damage a function of both S_i and $\frac{n_i}{N_i}$ rather than a single parameter [56]. The changes involving the S-N curve and endurance limit were considered sufficient modifications to permit a study of the criticisms of this method.

APPENDIX E

Mathematical Methods of Analysis

1. Equivalent Reversed Stress

Equation (E 1) was used to calculate the equivalent reversed stress, σ_G.

$$\sigma_G = \frac{\sigma_A}{1 - \frac{\sigma_M}{\sigma_F}} \qquad \text{(E 1)}$$

where σ_G = equivalent reversed stress, psi

σ_A = alternating stress, psi

σ_M = mean stress, psi

σ_F = true fracture stress, psi

Figure XII indicates the geometry of a modified Goodman diagram from which equation (E 1) is derived. The true fracture stress is used in lieu of the ultimate tensile strength in constructing the diagram as a result of work by Cina [4]. Cina's work showed that this procedure yields a more accurate value of equivalent reversed stress.

2. S-N Curves

The results of the constant load range and the completely reversed stress tests were analyzed by the method of linear regression. A best-fit line was obtained for the data on both S-log N and log S-log N coordinates. The limited number of test results required that statistical methods for small samples be used. Ninety-five per cent confidence limits were

FIGURE XII

MODIFIED GOODMAN DIAGRAM

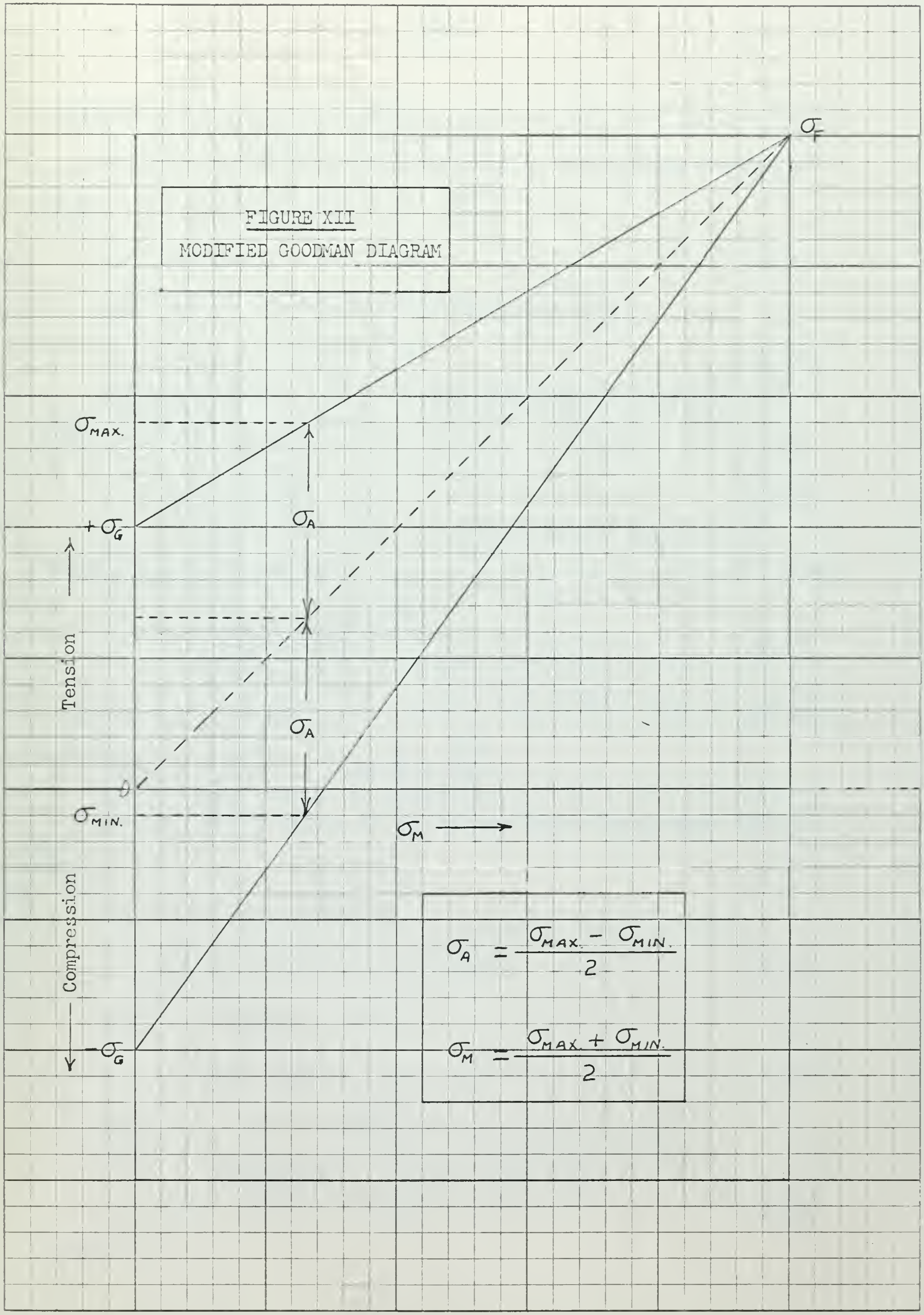

developed for each S-N curve.

For the straight regression line on log S-log N coordinates, the equation takes the form

$$SN^W = V \tag{E 2}$$

Equation (E 2) can be written in the form

$$\log S + W \log N = s \tag{E 3}$$

Designating $y = \log S$ as the independent variable and $x = \log N$ as the dependent variable, equation (E 3) becomes

$$y + wx = s \tag{E 4}$$

The coefficients w and s of the straight regression line are determined by

$$w = \frac{\sum xy - \sum x \sum y}{\sum x^2 - (\sum x)^2} \tag{E 5}$$

and $s = \bar{y} - w\bar{x}$ (E 6)

where $\bar{y} = \dfrac{\sum y}{n}$ and $\bar{x} = \dfrac{\sum x}{n}$

For any given value of y, 95 per cent confidence limits are found by

Upper confidence limit:

$$x_u = \frac{1}{w}\left[s - y + (t_{.5\alpha/\gamma})(\sqrt{\psi_s})\right] \tag{E 7}$$

Lower confidence limit:

$$x_l = \frac{1}{w}\left[s - y - (t_{.5\alpha/\gamma})(\sqrt{\psi_s})\right] \tag{E 8}$$

where ψ_s = modified sum of the squares, i.e.

$$\psi_s = \frac{\left(\dfrac{\sum y^2 - (\sum y)^2}{n} - w\left[\dfrac{\sum xy - (\sum x)(\sum y)}{n}\right]\right)}{n-2} \tag{E 9}$$

Values of $t_{(.5\alpha/\gamma)}$ corresponding to 95 per cent confidence and the degree of freedom, γ, are taken from tables of "Student's t-values for γ".

For this test $\alpha = .05$

$\gamma = n-2 = 8$

$t = 2.31$

The linear correlation coefficient, r, as given by the product moment formula is

$$r = \frac{\sum xy}{\sqrt{(\sum x^2)(\sum y^2)}} \qquad \text{(E 10)}$$

The procedure is the same for the S-log N regression line.

3. Standard Error of Estimate

The standard error of estimate provides a measure of deviation of the results of a prediction method from the actual values.

The standard error of estimate, ϵ , of Y on X is defined as

$$\epsilon = \sqrt{\frac{\sum (Y-Y_{est})^2}{N_d}} \qquad \text{(E 11)}$$

where Y_{est} represents the estimated value of Y for a given value of X.

For these tests Y was considered to be the actual number of cycles to failure as observed in the tests, and Y_{est} was the number of cycles predicted by a life prediction method or regression curve. N_d was the number of comparison points.

Thus the standard error of estimate for these tests took the form

$$\epsilon = \sqrt{\frac{\sum (N_{LT} - N_{LP})^2}{N_T}} \qquad \text{(E 12)}$$

where N_{LT} = number of cycles to failure, test

N_{LP} = number of cycles to failure, predicted

N_T = number of test data points

4. Degree of Conservatism

The predicted results were also compared with the actual test results by calculating the degree of conservatism for each method. The degree of conservatism, $\triangle$, is

$$\triangle = \frac{N_{LT}}{N_{LP}} \qquad \text{(E 13)}$$

If $\triangle < 1.00$, the prediction is unconservative.

If $\triangle \geq 1.00$, the prediction is conservative.

The values of the degree of conservatism, $\triangle$, were plotted on a log scale, Figure III, to take advantage of the fact that equal distances on each side of the ordinate of perfect correlation ($\triangle = 1.00$) represent equal degrees of conservatism.

APPENDIX F

Bibliography

1. Bell, W.J., and Benham, P.P., "The Effect of Mean Stress on Fatigue Strength of Plain and Notched Stainless Steel in the Range from 10 to 10^7 Cycles," ASTM Special Technical Publication No. 338, 1962, pp. 25-46.
2. Benham, P.P., "Fatigue of Metals Caused by a Relatively Few Cycles of High Load or Strain Amplitude," Metallurgical Reviews, Vol. 3, No. 11, 1958. pp. 203-234.
3. Bowler, A.H., and Lieberman, G.J., Engineering Statistics, Prentice-Hall, Inc., New Jersey, 1959.
4. Cina, B., "The Effect of Mode of Stressing in Fatigue Testing," Journal of the Iron and Steel Institute, March, 1960, pp. 332-337.
5. Coffin, L.F., Jr., "The Stability of Metals Under Cyclic Plastic Strain," Journal of Basic Engineering, Trans. ASME, Sept. 1960. pp. 671-682.
6. Corten, H.T., and Dolan, T.J., "Cumulative Fatigue Damage," Paper 2-Session 3, International Conference on Fatigue of Metals at the IME, Sept. 1956.
7. Daeves, K., Gerold, E., and Schulz, E.H., Stahl und Eisen, Vol. 60, 1940. p. 100.
8. DATMOBAS Confidential Report C-1665, "Proposed Engineering Concepts for Alleviating Fatigue Problems," January, 1964.

9. Dirkes, W., "An Analysis of Notched Uniaxial Fatigue Data," WADC TR-54-462, March 1955.

10. Dunham, F.W., "Fatigue Testing of Large-Scale Models of Submarine Structural Details," Paper, New England Section, SNAME, October 1964.

11. Enomoto, N., "A Method for Determining the Fatigue Limit of Metals by Means of Stepwise Load Increase Tests," ASTM Preprint No. 71, 1959.

12. Feltner, C.E., and Morrow, J., "Micro-Plastic Strain Hysteresis Energy as a Criterion for Fatigue Fracture," ASME Paper No. 60-MET-2, January 1960.

13. Freudenthal, A.M., "Cumulative Damage under Random Loading," Paper 4-Session 3, International Conference on Fatigue of Metals at the IME, Sept. 1956.

14. Freudenthal, A.M., and Heller, R.A., "On Stress Interaction in Fatigue and a Cumulative Damage Rule," Journal of the Aero/Space Sciences, Vol. 27, No. 7, July 1959.

15. Frost, N.E., and Phillips, C.E., Proceedings IME, Vol. 170, No. 21, 1956. p. 713.

16. Fuller, J.R., "Cumulative Fatigue Damage Due to Variable-Cycle Loading," Noise Control, July/August 1961, pp. 11-24.

17. Gatts, R.R., "Cumulative Fatigue Damage with Random Loading," Journal of Basic Engineering, Trans. ASME, Sept. 1962. pp. 403-409.

18. Gohn, G.R., Hardrath, H.F., and Peterson, R.E., "Fatigue of Metals," Materials Research and Standards, February 1963.

19. Gough, H.J., Symposium on Fatigue of Metals, Massachusetts Institute of Technology, 1950.

20. Gross, M.R., "Low-Cycle Fatigue of Materials (Laboratory Investigations)," USN Marine Engineering Laboratory, 1964.

21. Grover, H.J., "Cumulative Damage Theories," WADC TR-59-507, August 1959, pp. 2τ7-225.

22. Gunn, K., Aero. Quart., Vol. 6, 1955, p. 277.

23. Hanstock, R.F., Jour. Inst. Met., Vol. 83, 1954. p. 11.

24. Hartmann, A.J., et. a., "Effects of Weld Flaws on the Fatigue Behavior of Butt-Welded Joints in HY-80 Steel," Civil Eng. Dept., Univ. of Illinois Report Series No. 275, December 1963.

25. Head, A.K., and Hooke, F.H., Paper 9 - Session 3, International Conference on Fatigue of Metals at the IME, Sept. 1956.

26. Heller, R.A., Seki, M., and Freudenthal, A.M., "The Effects of Residual Stresses on Random Fatigue Life," ASTM Rreprint No. 67, 1964.

27. Henry, D.L., "A Theory of Fatigue Damage Accumulation in Steel," ASME Trans., Vol. 77, No. 6, August 1955. pp. 913-918.

28. Heywood, R.H., Stockholm Colloquium, 1955.

29. Hofmeister, W.F., "Use of Cumulative Damage Concepts," Metals Engineering Quarterly, November 1963.

30. Karius, A., Thesis, Carola Wilhelmia Technical School, Brunswick.

31. Kommers, J.B., "The Effect of Overstress in Fatigue on the Endurance Life of Steel," ASTM Proceedings, Vol. 45, 1945, pp. 532-541.

32. Kooistra, L.F., and Lemcoe, M.M., "Low-Cycle Fatigue Research on Full-Size Pressure Vessels," The Welding Journal, Vol. 41, No. 7, 1962, pp. 297-s to 306-s.

33. Langer, B.F., "Fatigue Failure from Stress Cycles of Varying Amplitude," Journal Applied Mechanics, Vol. 4, December 1937.

34. Langer, B.F., "Design of Pressure Vessels for Low-Cycle Fatigue," ASME Trans., Series D, Vol. 84, No. 3.

35. Levy, J.C., "Cumulative Damage in Fatigue - A Design Method Based on the S-N Curves," Journal Royal Aero. Society, Vol. 61, No. 559, July 1957, pp. 485-491.

36. Leybold, H.A., and Naumann, E.C., "A Study of Fatigue Life Under Random Loading," ASTM Preprint 70-B, June 1963.

37. Liu, H.W., and Corten, H.T., "Fatigue Damage Under Varying Stress Amplitudes," NASA TN D-647, November 1960.

38. Low-Cycle Fatigue Subcommittee, "Low-Cycle Fatigue," Mechanical Engineering, May 1963.

39. Lundberg, B., "Fatigue Life of Airplane," Journal of Aero Science, Vol. 22, No. 6, June 1955. pp. 349-402.

40. Manson, S.S., "Interpretive Report on Cumulative Fatigue Damage in the Low Cycle Range," Subcommittee on Plastic Fatigue Strength, PVRC, January 1963.

41. Manson, S.S., and Hirschberg, M.H., "Fatigue Behavior in Strain Cycling in the Low and Intermediate Cycle Range," 10th Sagamore Army Materials Research Conference.

42. Manson, S.S., Nachtigall, A.J., and Freche, J.C., "A Proposed New Relation for Cumulative Fatigue Damage in Bending," ASTM Proceedings, Vol. 61, 1961. pp. 679-703.

43. Marco, S.M., and Starkey, W.L., "A Concept of Fatigue Damage," ASME Trans., Vol. 76, No. 4, May 1954. pp. 627-632.

44. Metals Handbook, 8th Edition, Vol. 1, ASM, 1961.

45. Miner, M.A., "Cumulative Damage in Fatigue," Journal of Applied Mechanics, Trans. ASME, Vol. 12, No. 3, Sept. 1945, pp. A-159 to A-164.

46. Mordfin, L., and Halsey, N., "Programmed Maneuver-Spectrum Fatigue Tests of Aircraft Beam Specimens," ASTM Special Technical Publication No. 338, 1962. pp. 251 - 272.

47. NRL Report 6086, "Metallurgical Characteristics of High-Strength Structural Materials (3rd Quar. Report)," January 1964.

48. Noll, G.C., and Erickson, M.A., "Allowable Stresses for Steel Members of Finite Life," Proceedings SESA, Vol. 5, No. 2, 1948.

49. Palmgren, A., ZVDI, Vol. 68, 1924, p. 339.

50. Phillips, C.E., and Heywood, R.H., Proc. IME, Vol. 165, p. 113.

51. Pope, J.A., Metal Fatigue, Chapman and Hall, 1959.

52. Poppleton, E.D., "On the Prediction of Fatigue Life Under Random Loading," Inst. of Aerophysics, Univ. of Toronto, Report No. 82, February 1962.

53. Richart, F.E., Jr., and Newmark, N.M., "A Hypothesis for the Determination of Cumulative Damage in Fatigue," ASTM Proceedings, Vol. 48, 1948. pp. 767-798.

54. Rosenthal, D., and Sines, G., "Effect of Residual Stress on the Fatigue Strength of Notched Specimens," ASTM Proceedings, Vol. 51, 1951, p. 593.

55. Roylance, T.F., "A Review of Cumulative Damage in Fatigue," Ministry of Supply, S and T Memo No. 8/57, May 1957.

56. Schijve, J., and Jacobs, F.A., NLL (Holland) Report M. 1982, April 1955.

57. Schwab, R.C., "Cumulative Low-Cycle Fatigue Damage in HY-80 Steel (U)," U.S.N. Marine Engineering Laboratory Confidential Report 74/64, July 1964.

58. Shanley, F.R., "A Theory of Fatigue Based on Unbonding during Reversed Slip," RAND Corp. Report P-350-1, November, 1952.

59. Shanley, F.R., "A Theory of Fatigue Based on Unbonding during Reversed Slip: Supplement," RAND Corp. Report P-350-Supp., May 1953.

60. Shanley, F.R., "Fatigue Analysis of Aircraft Structures," RAND Corp. Paper No. RM1127, July 1953.

61. Smith, C.R., "Prediction of Fatigue Failures in Aluminum Alloy Structures," SESA Proceedings, Vol. 12, No. 2, 1955, pp. 21-28.

62. Valluri, S.R., "A Theory of Cumulative Damage in Fatigue," Office of Aerospace Research, ARL 182, December 1961.

63. Valluri, S.R., "Some Recent Developments at 'GALCIT' Concerning a Theory of Metal Fatigue," Acta Metallurgica, Vol. 11, No. 7, July 1963, pp. 759-775.

64. Wallgren, G., "Fatigue Tests with Stress Cycles of Varying Amplitude," FFA (Sweden) Report No. 48, 1953.

65. Weibull, W., Fatigue Testing and Analysis of Results, Pergamon Press, New York, 1961.

66. Yao, J.T.P., and Munse, W.H., "Low-Cycle Fatigue of Metals - Literature Review," Welding Research Supplement, April 1962. pp. 182-192.